Applied Energy xxx (2017) xxx–xxx

Contents lists available at ScienceDirect

Applied Energy

journal homepage: www.elsevier.com/locate/apenergy

# Multi-objective design optimization of distributed energy systems through cost and exergy assessments ☆

M. Di Somma [a,*], B. Yan [b], N. Bianco [c], G. Graditi [a], P.B. Luh [b], L. Mongibello [a], V. Naso [c]

[a] ENEA, Italian National Agency for New Technologies, Energy and Sustainable Economic Development, CR Portici, 80055 Portici, Italy
[b] Department of Electrical and Computer Engineering, University of Connecticut, Storrs, CT 06269, USA
[c] Dipartimento di Ingegneria Industriale (DII), Università degli studi Federico II, P.le Tecchio, Napoli 80125, Italy

## HIGHLIGHTS

- Exergy in design optimization of distributed energy systems (DESs).
- Multi-objective design optimization of DESs through cost and exergy assessments.
- Balancing solutions for planners based on economic and sustainability priorities.
- Cost and primary exergy of DESs reduced by 21–36% as compared with conventional systems.
- Exergy analysis for sustainable development of energy supply systems.

## ARTICLE INFO

*Article history:*
Received 13 January 2017
Received in revised form 6 March 2017
Accepted 22 March 2017
Available online xxxx

*Keywords:*
Distributed energy system
Design optimization
Multi-objective linear programming
Annual cost
Exergy efficiency

## ABSTRACT

In recent years, distributed energy systems (DESs) have been recognized as a promising option for sustainable development of future energy systems, and their application has increased rapidly with supportive policies and financial incentives. With growing concerns on global warming and depletion of fossil fuels, design optimization of DESs through economic assessments for short-run benefits only is not sufficient, while application of exergy principles can improve the efficiency in energy resource use for long-run sustainability of energy supply. The innovation of this paper is to investigate exergy in DES design to attain rational use of energy resources including renewables by considering energy qualities of supply and demand. By using low-temperature sources for low-quality thermal demand, the waste of high-quality energy can be reduced, and the overall exergy efficiency can be increased. The goal of the design optimization problem is to determine types, numbers and sizes of energy devices in DESs to reduce the total annual cost and increase the overall exergy efficiency. Based on a pre-established DES superstructure with multiple energy devices such as combined heat and power and PV, a multi-objective linear problem is formulated. In modeling of energy devices, the novelty is that the entire available size ranges and the variation of their efficiencies, capital and operation and maintenance costs with sizes are considered. The operation of energy devices is modeled based on previous work on DES operation optimization. By minimizing a weighted sum of the total annual cost and primary exergy input, the problem is solved by branch-and-cut. Numerical results show that the Pareto frontier provides good balancing solutions for planners based on economic and sustainability priorities. The total annual cost and primary exergy input of DESs with optimized configurations are reduced by 21–36% as compared with conventional energy supply systems, where grid power is used for the electricity demand, and gas-fired boilers and electric chillers fed by grid power for thermal demand. A sensitivity analysis is also carried out to analyze the influence of energy prices and energy demand variation on the optimized DES configurations.



## 1. Introduction

In recent years, depletion of fossil energy resources and global warming problems have prompted worldwide awareness about sustainability of energy supply. In such context, Distributed Energy Systems (DESs) have been recognized as a promising option for

☆ The short version of the paper was presented at ICAE2016 on Oct 8-11, Beijing, China. This paper is a substantial extension of the short version of the conference paper.

* Corresponding author.
*E-mail address:* marialaura.disomma@enea.it (M. Di Somma).

http://dx.doi.org/10.1016/j.apenergy.2017.03.105
0306-2619/

**Nomenclature**

| | |
|---|---|
| $A$ | area ($m^2$) |
| $c$ | constant in Eq. (34) (kW h/€) |
| $C$ | cost (€) |
| $C_c$ | specific capital cost (€/kW) - (€/kW h) - (€/$m^2$) |
| $C_{d,hr}$ | cooling rate (kW) |
| $COP$ | coefficient of performance |
| $CRF$ | capital recovery factor |
| $DR$ | maximum ramp-down rate (kW) |
| $D_t$ | length of the time interval (h) |
| $e$ | minimum part load |
| $E_{d,hr}$ | electricity rate (kW) |
| $ex_{Bio}$ | specific chemical exergy of biomass (kW h/kg) |
| $ex_{NG}$ | specific chemical exergy of natural gas (kW h/N $m^3$) |
| $Ex$ | exergy (kW h) |
| $Ex_{d,hr}$ | exergy rate (kW) |
| $F_{obj}$ | objective function |
| $F_q$ | Carnot factor |
| $G$ | natural gas volumetric flow rate (N $m^3$/h) |
| $H_{d,hr}$ | heating rate (kW) |
| $I$ | total solar irradiance (kW/$m^2$) |
| $LHV_{Bio}$ | lower heat value of biomass (kW h/kg) |
| $LHV_{NG}$ | lower heat value of natural gas (kW h/N $m^3$) |
| $n_i$ | total number of energy devices associated with technology $i$ |
| $N$ | lifetime (years) |
| $OM$ | O&M cost (€/kW h) |
| $P_{Bio}$ | biomass price (€/ton) |
| $P_e$ | electricity price (€/kW h) |
| $P_{NG}$ | natural gas price (€/N $m^3$) |
| $r$ | interest rate |
| $R_{d,hr}$ | energy rate (kW) |
| $S$ | designed size (kW) – (kW h) |
| $T$ | temperature (K) |
| $UR$ | maximum ramp-up rate (kW) |
| $x$ | binary decision variable |

*Greek symbols*

| | |
|---|---|
| $\varepsilon_{gen}$ | exergy efficiency of electricity generation |
| $\varsigma_{FUEL}$ | exergy factor of fuel |
| $\eta$ | efficiency |
| $\varphi$ | storage loss fraction |
| $\psi$ | overall exergy efficiency |
| $\omega$ | weight in Eq. (34) |

*Superscript/subscripts*

| | |
|---|---|
| 0 | reference |
| *Abs* | absorption chiller |
| *ASHP* | air source heat pump |
| *Bio* | biomass |
| *Bioboil* | biomass boiler |
| *CHP NGICE* | combined heat and power with gas-fired internal combustion engine |
| *CHP NGMTG* | combined heat and power with gas-fired micro-turbine |
| *coll* | collector |
| *d* | day |
| *dem* | demand |
| *DHW* | domestic hot water |
| *e* | electricity |
| *ES* | electrical storage |
| *FUEL* | fuel |
| *GRID* | power grid |
| *hr* | hour |
| *i* | index of technology |
| *in* | input |
| *INV* | investment |
| *j* | energy carrier |
| *l* | range |
| $k_i$ | energy device associated with technology $i$ |
| $K_i$ | maximum number of energy devices associated with technology $i$ |
| max | maximum |
| min | minimum |
| *NG* | natural gas |
| *NGboil* | gas-fired boiler |
| *O&M* | operation and maintenance |
| *out* | output |
| *PV* | photovoltaic |
| *req* | required |
| *SC* | space cooling |
| *SH* | space heating |
| *SOLAR* | solar |
| *ST* | solar thermal |
| *sto* | stored |
| *TES* | thermal energy storage |
| *th* | thermal |
| *TOT* | total |

*Acronyms*

| | |
|---|---|
| *CHP* | combined heat and power |
| *DES* | distributed energy system |
| *MOLP* | multi-objective linear programming |
| *O&M* | operation and maintenance |

sustainable development of future energy systems [1–6]. A DES refers to a multi-input and multi-output energy system, consisting of multiple small-scale technologies, including renewable ones and storage units, providing electric and thermal energy close to end-users [1–8]. Therefore, as compared with conventional energy supply systems, DESs may employ a wide range of technologies, thereby offering the possibility to integrate renewables as well as to recover waste heat from power generation processes for thermal purposes in buildings [2–4]. The application of DESs has increased rapidly in recent years with the supportive government policies and financial incentives [1,3,4,8]. However, to achieve the expected potentials of DESs, it is necessary to determine the system configuration rationally by selecting the appropriate energy devices, and identifying their numbers and sizes, and the corresponding operation strategies, to match energy requirements of a specific end-user [2,9–11]. Design optimization of a DES is therefore essential for future energy planning, and inherently involves multiple and conflicting objectives [12–15]. For instance, the interest of DES developers in achieving a system configuration with lowest costs might conflict with the interest of energy legislations such as the EU ones in increasing sustainability of energy supply, which can be attained by reducing the waste of fossil energy resources and environmental impacts [15,16]. In such a context, a multi-objective approach helps identify balancing solutions to promote participation in the decision-making process and facilitate collective decisions [12].

According to [16], application of exergy principles in building energy supply systems may promote rational use of energy resources, by taking into account the different energy quality levels of energy supply and those of building demand. Electrical and

Please cite this article in press as: Di Somma M et al. Multi-objective design optimization of distributed energy systems through cost and exergy assessments. Appl Energy (2017), http://dx.doi.org/10.1016/j.apenergy.2017.03.105

chemical energy are high-quality energy, whereas low-temperature heat is low-quality energy. In current energy supply systems, energy is commonly supplied as electricity or as fossil energy carriers, whose energy quality is unnecessarily high to meet low-quality thermal demand in buildings, and the First Law of Thermodynamics does not consider the energy quality degradation occurring in such processes. Conversely, based on the Second Law of Thermodynamics, by reducing the supply of high-quality energy for thermal demand in buildings through the usage of low-temperature sources, efficient use of the potential (i.e., quality) of the energy resources is promoted. Since energy resources, and particularly fossil fuels, are limitedly available, better exploiting their potential allows to reduce their waste. In this way, lifetime of fossil fuels can be extended, and the environmental impacts derived from their use can be reduced [16]. In the literature, exergy analysis has been linked to sustainability of energy supply which is essential for the long run, since it clearly identifies the efficiency in energy resource use, by considering their potential; and the importance of including exergy in energy legislations was discussed [16–21]. Exergy was investigated in performance evaluation of single energy supply systems, as cogeneration systems [22–25], renewable energy sources [26,27], various types of heat pumps [28–30], and thermal energy storage [31–33] with the aim to reduce energy quality degradation in designing and managing these systems, thereby improving sustainability of energy supply. DESs provide a great opportunity to demonstrate the effectiveness of exergy analysis in designing more sustainable energy systems since multiple energy resources with different energy quality levels can be used to satisfy user various demand with different quality levels. By using low exergy sources, e.g., solar thermal or waste heat of power generation, for low-quality thermal demand, and high exergy sources for electricity demand, the waste of high-quality energy can be reduced, thereby increasing the overall exergy efficiency of DESs.

In previous work, exergy modeling and optimization were investigated in DES operations through a multi-objective approach [34,35]. Based on fixed DES configurations (types, numbers and sizes of energy devices), optimized operation strategies were established by considering energy costs and exergy efficiency. As for design optimization of DESs, most studies in the literature focused on minimizing the total annual cost (annualized investment costs and annual operating costs of the system) as a crucial objective for DES developers [2,36–42]. Beyond minimizing costs only, design optimization of DESs through multi-objective approach to reduce also environmental impact was analyzed. In [43], a multi-objective linear programming (MOLP) model was established to find the optimal configuration and operation of a DES for an industrial area while reducing the total annual cost and $CO_2$ emission. The problem was solved by using the compromise programming method. In [44], a MOLP model was developed to optimally design and operate an energy system consisting of buildings equipped with small-size Combined Heat and Power (CHP) plants, with the aim to reduce both annual costs and $CO_2$ emission. In [45], a general framework was developed to study the application of energy hubs for determining the optimal design and operation of DESs in urban areas according to economic and environmental objectives, and the multi-objective optimization problem was solved by using branch-and-cut. In all the analyzed works, before optimizing the design, "superstructures" were pre-established with energy devices chosen among the most commonly used ones in practical DESs. Moreover, to identify the size of an energy device, several sizes were pre-fixed as possible choices to be selected through binary decision variables [2,36–40,44,45]. However, it is difficult to select the sizes among the almost infinite possible solutions available in the market. Conversely, the size of an energy device was a continuous decision variable within the entire available size range, with efficiencies as well as specific capital and operation and maintenance (O&M) costs assumed constant in the entire size range and their variations with the sizes were not considered [41,42]. The size of an energy device was a continuous decision variable within the entire available size range in [43], with prices and efficiencies approximated as linear functions of the size.

The innovation of this paper is to investigate exergy in DES design optimization through a multi-objective approach to attain rational use of energy resources considering economic and sustainability priorities. A superstructure is pre-established with multiple energy devices, such as CHPs with natural gas-fired internal combustion engines and micro-turbines as prime movers, natural gas and biomass boilers, solar thermal collectors, PV, reversible air-source heat pumps, single-stage absorption chillers, and electrical and thermal energy storage devices. Given user demand includes electricity, domestic hot water, space heating, and space cooling. To take both cost and exergy assessments into account, a MOLP problem is formulated, and the goal is to determine types, numbers and sizes of energy devices in the DES with the corresponding operation strategies on the Pareto frontier, thereby providing different design options for planners based on short- and long-run priorities. In modeling of energy devices, the key novelty is that the entire size ranges available in the market as well as the variations of efficiencies, specific capital and O&M costs with sizes are taken into account, based on a detailed market analysis. These characteristics are usually piecewise linear functions of the device size, which is a continuous decision variable, thereby making the problem nonlinear. To maintain the problem linearity, the key idea is to divide the entire size range of an energy device into several small ranges, so that these characteristics can be assumed constant in each size range. The daily operation of energy devices is modeled based on previous work on operation optimization of DESs [34]. The economic objective is formulated as the total annual cost (total annualized investment cost, total annual O&M and energy cost) to be minimized. The exergetic objective is to maximize the overall exergy efficiency of the DES, defined as the ratio of the total annual exergy required to meet the given energy demand to the total annual primary exergy input to the system. Assuming known the energy demand, the total exergy required to meet the demand is also known. Therefore, the exergetic objective is formulated as the total annual primary exergy input to be minimized. By minimizing a weighted sum of the total annual cost and primary exergy input, the problem is solved by branch-and-cut. The general mathematical formulation established and the optimization method provided could be applicable in real contexts, thereby providing decision support to planners. Given the input data, such as end-user demand, local climate data, energy prices and technical and economic information of the candidate energy devices, the model allows to obtain their optimized combination, and the corresponding operation strategies through cost and exergy assessments. As an illustrative example, the model is implemented for a hypothetic building cluster located in Italy. The optimization is carried out on an hourly basis for four representative season days. Numerical results demonstrate that exergy analysis is a powerful tool for designing more sustainable energy supply systems based on the use of renewables and low-temperature sources for thermal demand in buildings, and that good balancing options for planners are found on the Pareto frontier. Moreover, the total annual cost and primary exergy input of DESs with optimized configurations are significantly reduced, by 21–36% as compared with conventional energy supply systems, where grid power is used for the electricity demand, natural gas boilers for domestic hot water and space heating demand, and electric chillers fed by grid power for space cooling demand. In addition, a sensitivity analysis is carried out to analyze the influence of key parameters such as energy

Please cite this article in press as: Di Somma M et al. Multi-objective design optimization of distributed energy systems through cost and exergy assessments. Appl Energy (2017), http://dx.doi.org/10.1016/j.apenergy.2017.03.105

prices and energy demand variation on the optimized DES configurations and the related economic and exergetic performances.

In the following, Section 2 is on the problem formulation and the optimization method. Numerical testing is presented and discussed in Section 3. Sensitivity analysis is presented in Section 4.

## 2. Problem formulation and optimization method

The superstructure of the DES under consideration is shown in Fig. 1. The energy devices are chosen among the most commonly used ones in practical DESs.

Electricity demand and electricity required by heat pumps can be satisfied by grid power, by the electricity provided by CHPs with natural gas-fired internal combustion engines and micro-turbines as prime movers, PV, and by the electricity discharged from the electrical storage. It is assumed that all the electricity provided by CHPs and PV is self-consumed, while no extra electricity is sold back to the power grid. Domestic hot water demand can be satisfied by thermal energy provided by CHPs, natural gas and biomass boilers, solar thermal collectors, and by thermal energy discharged from the storage. Space heating demand can be satisfied by thermal energy provided by CHPs, natural gas and biomass boilers, heat pumps, and by thermal energy discharged from the storage. Space cooling demand can be satisfied by thermal energy provided by CHPs, natural gas and biomass boilers through the absorption chillers, heat pumps, and by thermal energy discharged from the storage.

In the following, the decision variables are first introduced in Section 2.1. The economic and exergetic objectives are presented in nd 2.22.3, respectively. The constraints are established in Section 2.4. The optimization method is discussed in Section 2.5.

### 2.1. Decision variables

In the optimization problem, the decision variables include: existence, numbers, and sizes of energy devices; operation status (on/off) and energy rates provided by energy devices; capacities of electrical and thermal storage devices; electricity and heat rate input and output to/from electrical and thermal storage devices, respectively; and electricity rate bought from the power grid. Existence and operation status of energy devices are binary. Numbers of energy devices are also determined through binary decision variables to be explained later. All the other decision variables are continuous.

### 2.2. Economic objective

The economic objective is to minimize the total annual cost of the DES, $C_{TOT}$, formulated as the sum of the total annualized investment cost, and the total annual O&M and energy costs:

$$C_{TOT} = C_{INV} + C_{O\&M} + C_{FUEL} + C_{GRID}, \tag{1}$$

where $C_{INV}$ is the annualized investment cost of all energy devices in the DES; $C_{O\&M}$ is the total annual O&M cost of all energy devices; $C_{FUEL}$ is the total annual cost of consumed fuels; and $C_{GRID}$ is the annual cost of purchasing electricity from the power grid.

The total annualized investment cost of the energy devices is formulated as:

$$C_{INV} = \sum_{i} \sum_{k_i}^{K_i} CRF_i \left(C_{c,i} S_{i,k_i}\right),$$
$$CRF_i = r(1+r)^{N_i} / \left[(1+r)^{N_i} - 1\right], \tag{2}$$

where $CRF_i$ is the capital recovery factor of technology $i$; $K_i$ is the maximum number of energy devices associated with technology $i$, which is assumed to be known; $k_i$ is the energy device associated with technology $i$; $S_{i,k_i}$ is the designed size of device $k_i$; $C_{c,i}$ is the specific capital cost; $r$ is the interest rate; and $N_i$ is the lifetime. The size of electrical and thermal energy storage devices represents the capacity expressed in kW h, and the specific capital cost is expressed in €/kW h. The size of the solar thermal collectors is expressed in terms of the total surface of collectors to be installed, and the specific capital cost is expressed in €/m$^2$.

The total annual O&M cost of energy devices is formulated as:

$$C_{O\&M} = \sum_{i} \sum_{k_i}^{K_i} \sum_{d} \sum_{hr} OM_i R_{i,k_i,d,hr} D_t, \tag{3}$$

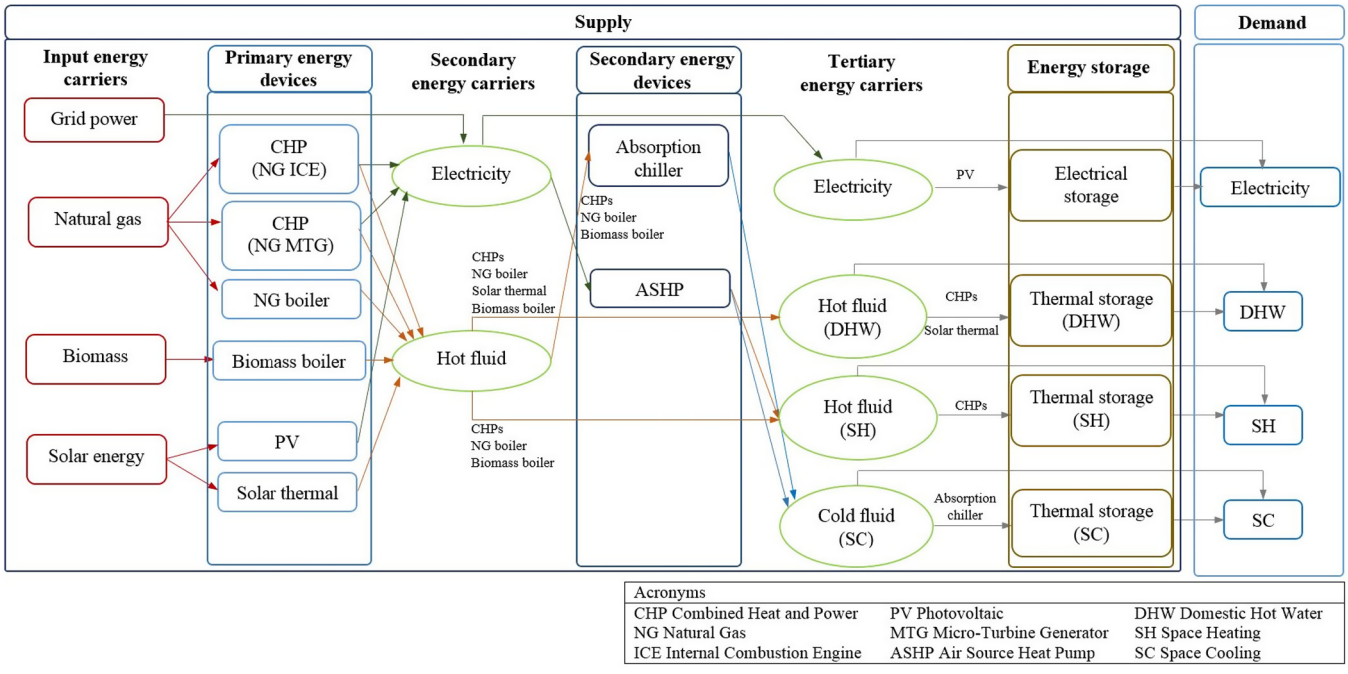


**Fig. 1.** Superstructure representation of the DES for the design optimization problem.

Please cite this article in press as: Di Somma M et al. Multi-objective design optimization of distributed energy systems through cost and exergy assessments. Appl Energy (2017), http://dx.doi.org/10.1016/j.apenergy.2017.03.105

where $OM_i$ is the O&M cost of the technology $i$; $R_{i,k_i,d,hr}$ is the energy rate provided by the energy device $k_i$ at hour $hr$ of day $d$; and $D_t$ is the length of the time interval (1 h). For electrical and thermal storage devices, the O&M costs are based on their capacities.

The total annual cost of the consumed fuels is formulated as:

$$C_{FUEL} = \sum_{i\in\{CHP\,NGICE,\ CHP\,NGMTG,\ NG\,boil\}} \sum_{k_i}^{K_i} \sum_{d} \sum_{hr} P_{NG}\left(R_{i,k_i,d,hr}/(\eta_i LHV_{NG})\right) D_t + \sum_{i\in\{Bioboil\}} \sum_{k_i}^{K_i} \sum_{d} \sum_{hr} P_{Bio}\left(R_{i,k_i,d,hr}/(\eta_i LHV_{Bio})\right) D_t, \quad (4)$$

where $\eta_i$ is the energy efficiency (thermal or electrical); $P_{NG}$ and $P_{Bio}$ are the price of natural gas and biomass, respectively; and $LHV_{NG}$ and $LHV_{Bio}$ are the lower heat value of natural gas and biomass, respectively.

The annual cost of purchased grid power is formulated as:

$$C_{GRID} = \sum_{d}\sum_{hr} P_{e,hr} E_{GRID,d,hr} D_t, \quad (5)$$

where $P_{e,hr}$ is the time-of-day unit price of electricity from the power grid, and $E_{GRID,d,hr}$ is the electricity rate taken from the grid.

### 2.3. Exergetic objective

The exergetic objective is to maximize the overall exergy efficiency of the DES, $\psi$, defined as the ratio of the total annual exergy output, $Ex^{out}$, to the total annual primary exergy input, $Ex_{in}$ [34,46,47]:

$$\psi = Ex^{out}/Ex_{in}. \quad (6)$$

The total annual exergy output is the total annual exergy required to meet the given user demand in the whole year, formulated as:

$$Ex^{out} = \sum_{dem}\sum_{d}\sum_{hr} Ex^{dem}_{d,hr} D_t, \quad dem \in \{e, DHW, SH, SC\}, \quad (7)$$

where $Ex^{dem}_{d,hr}$ is the total exergy rate required to meet the electricity and thermal demand (domestic hot water, and space heating and cooling). In buildings, energy demands are characterized by different energy quality levels. To meet the electricity demand, the highest quality of energy is needed. The exergy rate required to meet the electricity demand, $Ex^{e}_{d,hr}$, can be evaluated as follows [34,35,48]:

$$Ex^{e}_{d,hr} = E^{e}_{d,hr}, \quad \forall d, \forall hr, \quad (8)$$

where $E^{e}_{d,hr}$ is the electricity demand rate.

As for thermal demand, the energy quality depends on temperature required – the lower the temperature required, the lower the exergy [16,48]. The exergy rate required to meet the demand of domestic hot water can be formulated as:

$$Ex^{DHW}_{d,hr} = H^{DHW}_{d,hr} F^{DHW}_{q,d,hr}, \quad \forall d, \forall hr, \quad (9)$$

where $H^{DHW}_{d,hr}$ is the heat demand rate for domestic hot water, and $F^{DHW}_{q,d,hr}$ is the Carnot factor, formulated as [16,34,35,48]:

$$F^{DHW}_{q,d,hr} = 1 - T_{0,d,hr}/T^{DHW}_{req}, \quad \forall d, \forall hr, \quad (10)$$

which depends on both the temperature required for the domestic hot water, $T^{DHW}_{req}$, which is assumed to be known based on [49], and the reference temperature, $T_{0,d,hr}$, assumed to be known as the averaged ambient temperature at hour $hr$ of day $d$ [16,34]. The exergy rate required to meet the demand of space heating and cooling can be formulated similarly.

At the supply side, the input energy carriers are grid power, natural gas, biomass, and solar energy. The total annual primary exergy input is formulated as:

$$Ex_{in} = \sum_{j}\sum_{d}\sum_{hr} Ex_{j,d,hr} D_t, \quad j \in \{GRID, FUEL, SOLAR\}, \quad (11)$$

where $Ex_{j,d,hr}$ is the exergy rate input to the DES related to the energy carrier $j$. As well as for the demand side, also the supply side is characterized by different energy quality levels.

Electricity from the power grid is an energy carrier provided by power generation plants, and the exergy input rate to the DES, $Ex_{GRID,d,hr}$, depends on the exergy efficiency of the plants, $\varepsilon_{gen}$ [34,35]:

$$Ex_{GRID,d,hr} = E_{GRID,d,hr}/\varepsilon_{gen}, \quad \forall d, \forall hr, \quad (12)$$

The exergy input rates of fuels (natural gas and biomass) depend on their specific chemical exergy:

$$Ex_{FUEL,d,hr} = \sum_{i\in\{CHP\,NGICE,\ CHP\,NGMTG,\ NGboil\}} \sum_{k_i}^{K_i} ex_{NG}(R_{i,k_i,d,hr}/(\eta_i LHV_{NG})) + \sum_{i\in\{Bioboil\}} \sum_{k_i}^{K_i} ex_{Bio}(R_{i,k_i,d,hr}/(\eta_i LHV_{Bio})),$$
$$ex_{FUEL} = \varsigma_{FUEL} LHV_{FUEL}, \quad FUEL \in \{NG, Bio\}, \forall d, \forall hr, \quad (13)$$

where $ex_{FUEL}$ is the specific chemical exergy of the fuel, and $\varsigma_{FUEL}$ is the exergy factor [50].

As for solar energy, thermal energy output of the solar thermal collectors at the corresponding temperature levels, and electricity output of PV are considered as the primary energy sources [51,52], respectively. The exergy input rate to solar thermal collectors, $Ex_{ST,d,hr}$, is formulated as:

$$Ex_{ST,d,hr} = H_{ST,d,hr}(1 - T_{0,d,hr}/T^{out}_{coll}), \ \forall d, \ \forall hr, \quad (14)$$

where $H_{ST,\,d,\,hr}$ is the heat rate provided by solar thermal collectors, and $T_{0,d,hr}$ and $T^{out}_{coll}$ are the reference temperature, assumed as the averaged ambient temperature at hour $h$ of day $d$ [16,34], and the temperature of the heat transfer fluid at the exit of the collector field (assumed constant), respectively.

The exergy input rate to PV, $Ex_{PV,d,hr}$, is formulated as:

$$Ex_{PV,d,hr} = E_{PV,d,hr}, \quad \forall d, \ \forall hr. \quad (15)$$

where $E_{PV,\,d,\,hr}$ is the electricity rate provided by PV.

Therefore, the exergy rate of solar energy input to the DES is formulated as:

$$Ex_{SOLAR,d,hr} = Ex_{ST,d,hr} + Ex_{PV,d,hr}, \quad \forall d, \forall hr. \quad (16)$$

Since energy demand as well as the temperatures required for the demand of domestic hot water, and space heating and cooling are assumed known, the total exergy required to meet the demand is also known, and the overall exergy efficiency can be increased by reducing the total primary exergy input. Therefore, the exergetic objective is formulated as the total annual primary exergy input to the DES to be minimized as in Eq. (11).

### 2.4. Constraints

The constraints in the optimization problem include design constraints, energy balances and operation constraints, as discussed below.

Please cite this article in press as: Di Somma M et al. Multi-objective design optimization of distributed energy systems through cost and exergy assessments. Appl Energy (2017), http://dx.doi.org/10.1016/j.apenergy.2017.03.105

*2.4.1. Design constraints*

The designed size of the energy device $k_i$ has to be within the minimum and maximum sizes of the related technology $S_i^{\min}$ and $S_i^{\max}$ available in the market:

$$S_i^{\min} x_{i,k_i} \leqslant S_{i,k_i} \leqslant S_i^{\max} x_{i,k_i}, \quad k_i \leqslant K_i, \quad n_i = \sum_{k_i}^{K_i} x_{i,k_i}, \quad \forall i, \tag{17}$$

where $x_{i,k_i}$ is a binary decision variable, which is equal to 1 if the device $k_i$ is implemented in the DES configuration; and $n_i$ is the total number of energy devices associated with technology $i$ implemented in the DES configuration. As for solar collector and PV arrays, the total designed area has to be lower than the available one. In the design optimization problem, the entire size range available in the market as well as the variations of efficiencies, specific capital and O&M costs with sizes, are taken into account. These characteristics are usually piecewise linear functions of the size, which is a continuous decision variable, thereby making the problem nonlinear. To avoid this, the key idea is to divide the entire size range of an energy device into several small ranges, so that these characteristics can be assumed constant in each size range. Consider CHP with a natural gas-fired internal combustion engine as an example. The designed size of CHP in range $l$ is limited by its minimum and maximum values $S_{CHP\,NGICE}^{\min,l}$ and $S_{CHP\,NGICE}^{\max,l}$ in this range:

$$S_{CHP\,NGICE}^{\min,l} x_{k_{CHP\,NGICE}}^{l} \leqslant S_{k_{CHP\,NGICE}}^{l} \leqslant S_{CHP\,NGICE}^{\max,l} x_{k_{CHP\,NGICE}}^{l},$$
$$\sum_{l} x_{k_{CHP\,NGICE}}^{l} \leqslant 1, \quad \forall l, k_{CHP\,NGICE} \leqslant K_{CHP\,NGICE}, \tag{18}$$

where $S_{k_{CHP\,NGICE}}^{l}$ and $x_{k_{CHP\,NGICE}}^{l}$ are defined similarly as in Eq. (17) in range $l$. Also the summation of binary decision variables $x_{k_{CHP\,NGICE}}^{l}$ over $l$ has to be smaller than or equal to 1, ensuring that at most one range can be selected for each energy device associated to each technology.

*2.4.2. Energy balances*

To satisfy the given user demand, electricity, domestic hot water, and space heating and cooling energy balances are formulated in the following.

For electricity, the sum of the electricity demand and the total electricity required by the reversible air source heat pumps has to be satisfied by the sum of the total electricity provided by CHPs, PV, grid power, and electrical storage:

$$E_{d,hr}^{e} + \sum_{k_{ASHP}} E_{k_{ASHP},d,hr} = E_{PV,d,hr} + \sum_{k_{CHP\,NGICE}} E_{k_{CHP\,NGICE},d,hr} + \sum_{k_{CHP\,NGMTG}} E_{k_{CHP\,NGMTG},d,hr} + E_{GRID,d,hr} + E_{ES,d,hr}^{e,out} - E_{ES,d,hr}^{e,in}, \quad \forall d, hr, \tag{19}$$

where $E_{ES,d,hr}^{e,out}$ and $E_{ES,d,hr}^{e,in}$ are the electricity rates discharged and charged from/to the storage, respectively, which are both continuous decision variables.

For the domestic hot water demand, the demand has to be satisfied by the total thermal energy provided by CHPs, natural gas and biomass boilers, solar thermal collectors, and thermal storage:

$$H_{d,hr}^{DHW} = \sum_{k_{CHP\,NGICE}} H_{k_{CHP\,NGICE},d,hr}^{DHW} + \sum_{k_{CHP\,NGMTG}} H_{k_{CHP\,NGMTG},d,hr}^{DHW} + \sum_{k_{NGboil}} H_{k_{NGboil},d,hr}^{DHW} + \sum_{k_{Bioboil}} H_{k_{Bioboil},d,hr}^{DHW} + H_{ST,d,hr} + H_{TES,d,hr}^{DHW,out} - H_{TES,d,hr}^{DHW,in}, \quad \forall d, hr, \tag{20}$$

where $H_{TES,d,hr}^{DHW,out}$ and $H_{TES,d,hr}^{DHW,in}$ are the heat rates discharged and charged from/to the storage, respectively, which are both continuous decision variables.

The space heating and space cooling energy balances are formulated in a similar way.

*2.4.3. Operation constrains*

For most of the energy devices included in the DES superstructure, the common constraint is the capacity constraint. The energy rate provided by each energy device is limited by its minimum part load and the capacity, if the device is on. Still considering the CHP with a natural gas-fired internal combustion engine as an example, the electricity rate, $E_{k_{CHP\,NG\,ICE},d,hr}$, is limited by the minimum and maximum rated output $E_{k_{CHP\,NG\,ICE}}^{\min}$ and $E_{k_{CHP\,NG\,ICE}}^{\max}$, if the device is on:

$$E_{k_{CHP\,NG\,ICE}}^{\min} x_{k_{CHP\,NG\,ICE},d,hr} \leqslant E_{k_{CHP\,NG\,ICE},d,hr} \leqslant E_{k_{CHP\,NG\,ICE}}^{\max} x_{k_{CHP\,NG\,ICE},d,hr}, \quad \forall k_{CHP\,NGICE}, \quad \forall d, hr, \tag{21}$$

where $x_{k_{CHP\,NG\,ICE},d,hr}$ is the on/off status of CHP. The minimum part load and the maximum rated output are obtained based on the design capacity of CHP as follows:

$$E_{k_{CHP\,NG\,ICE}}^{\min} = e_{k_{CHP\,NG\,ICE}} \sum_{l} S_{k_{CHP\,NG\,ICE}}^{l}, \quad E_{k_{CHP\,NG\,ICE}}^{\max} = \sum_{l} S_{k_{CHP\,NG\,ICE}}^{l}, \quad \forall k_{CHP\,NG\,ICE}, \tag{22}$$

where $e_{k_{CHP\,NG\,ICE}}$ is the minimum part load expressed in percentage of the designed size. The product of one continuous and one binary decision variables is linearized in a standard way [53].

In the following, the additional constraints of each energy device are presented.

*2.4.3.1. CHP systems.* Two types of CHPs are involved in the DES superstructure, i.e., CHPs with gas-fired internal combustion engine and with micro-turbines. They consist of prime movers to meet the electricity load, and heat recovery units providing thermal energy to meet the demand of domestic hot water and space heating, and to meet the demand of space cooling through absorption chillers. Operation constraints for CHPs with gas-fired internal combustion engine as prime mover are presented below.

The ramp rate constraint limits the variations in the power generation between two successive time steps to be within the ramp-down, $DR_{k_{CHP\,NGICE}}$, and ramp-up, $UR_{k_{CHP\,NGICE}}$ [34,54]:

$$DR_{k_{CHP\,NGICE}} \leqslant E_{k_{CHPNGICE},d,hr} - E_{k_{CHPNGICE},d,hr-1} \leqslant UR_{k_{CHPNGICE}}, \quad \forall k_{CHP\,NG\,ICE}, \quad \forall d, hr, \tag{23}$$

where the ramp-down and the ramp-up and are expressed in percentage of the designed size.

The volumetric flow rate of natural gas, $G_{k_{CHP\,NGICE},d,hr}$, required by the CHP to provide the electricity rate, $E_{k_{CHP\,NG\,ICE},d,hr}$, is formulated as:

$$G_{k_{CHP\,NGICE},d,hr} = E_{k_{CHP\,NGICE},d,hr} / (\eta_{e,k_{CHP\,NGICE}} LHV_{NG}), \quad \forall k_{CHP\,NGICE}, \quad \forall d, hr. \tag{24}$$

In the above, $\eta_{e,k_{CHP\,NGICE}}$ is the electrical efficiency of the CHP, formulated as:

$$\eta_{e,k_{CHP\,NGICE}} = \sum_{l} x_{k_{CHP\,NGICE}}^{l} \eta_{e,k_{CHP\,NGICE}}^{l}, \quad \forall k_{CHP\,NGICE}, \tag{25}$$

where $\eta_{e,k_{CHP\,NGICE}}^{l}$ is the electrical efficiency of the CHP in the range $l$.

The heat rate recovered from the CHP, $H_{k_{CHP\,NGICE},d,hr}$, is formulated as:

$$H_{k_{CHP\,NGICE},d,hr} = E_{k_{CHP\,NGICE},d,hr} \eta_{th,k_{CHP\,NGICE}} / \eta_{e,k_{CHP\,NGICE}}, \quad \forall k_{CHP\,NGICE}, \quad \forall d, hr, \tag{26}$$

where $\eta_{th,k_{CHP\,NGICE}}$ is the thermal efficiency of the CHP defined similarly as in Eq. (25).

Please cite this article in press as: Di Somma M et al. Multi-objective design optimization of distributed energy systems through cost and exergy assessments. Appl Energy (2017), http://dx.doi.org/10.1016/j.apenergy.2017.03.105

The heat rate recovered by CHP is subdivided to meet the demand of domestic hot water and space heating, and to meet the demand of space cooling through the absorption chillers:

$$H_{k_{CHP\,NGICE},d,hr} = H^{DHW}_{k_{CHP\,NGICE},d,hr} + H^{SH}_{k_{CHP\,NGICE},d,hr} + H^{SC}_{k_{CHP\,NGICE},d,hr}, \quad \forall k_{CHP\,NGICE}, \quad \forall d, hr. \tag{27}$$

Constraints for CHPs with micro-turbines as prime movers are similar to those formulated above.

*2.4.3.2. Boilers.* Natural gas and biomass boilers may be involved to meet the demand of domestic hot water, space heating, and to meet the demand of space cooling through absorption chillers. Operation constraints for gas-fired boilers are presented below.

The volumetric flow rate of natural gas, $G_{k_{NGBoil},d,hr}$, required by the gas-fired boiler to provide the heat rate, $H_{k_{NGBoil},d,hr}$, is formulated as:

$$G_{k_{NGBoil},d,hr} = H_{k_{NGBoil},d,hr}/(\eta_{th,k_{NGBoil}} LHV_{NG}), \quad \forall k_{NGBoil}, \quad \forall d, hr, \tag{28}$$

where $\eta_{th,k_{NGBoil}}$ is the thermal efficiency of the boiler defined similarly as in Eq. (25). The heat rate provided by the boiler is subdivided to meet the demand of domestic hot water and space heating, and to meet the demand of space cooling through the absorption chillers:

$$H_{k_{NGBoil},d,hr} = H^{DHW}_{k_{NGBoil},d,hr} + H^{SH}_{k_{NGBoil},d,hr} + H^{SC}_{k_{NGBoil},d,hr}, \quad \forall k_{k_{NGBoil}}, \quad \forall d, hr. \tag{29}$$

Constraints for biomass boilers are similar to those formulated above.

*2.4.3.3. Solar energy systems.* Solar PV and solar thermal collectors may be involved to meet the electricity load and the domestic hot water demand, respectively.

The electricity rate provided by solar PV, $E_{PV,d,hr}$, is formulated as [36,55]:

$$E_{PV,d,hr} = A_{PV}\eta_{PV} I_{d,hr}, \quad \forall d, hr, \tag{30}$$

where $A_{PV}$ is the total area to be installed, $\eta_{PV}$ is the electrical efficiency, and $I_{d,hr}$ is the hourly solar irradiance in day $d$.

The heat rate provided by solar thermal collectors can be expressed in a similar way.

*2.4.3.4. Absorption chiller.* Absorption chillers may be involved to meet the demand of space cooling, powered by the total thermal energy recovered from CHPs, and provided by natural gas and biomass boilers. The cooling rate provided by the absorption chiller, $C_{k_{Abs},d,hr}$, is expressed as:

$$C_{k_{Abs},d,hr} = \left( \sum_{k_{CHP\,NGICE}} H^{SC}_{k_{CHP\,NGICE},d,hr} + \sum_{k_{CHP\,NGMTG}} H^{SC}_{k_{CHP\,NGMTG},d,hr} + \sum_{k_{NGboil}} H^{SC}_{k_{NGboil},d,hr} + \sum_{k_{Bioboil}} H^{SC}_{k_{Bioboil},d,hr} \right) COP_{k_{Abs}}, \quad \forall k_{Abs}, \quad \forall d, hr, \tag{31}$$

where $COP_{k_{Abs}}$ is the coefficient of performance of the absorption chiller defined similarly as in Eq. (25).

*2.4.3.5. Reversible air source heat pump.* Reversible air source heat pumps may be involved to meet the space heating and cooling demand in heating and cooling mode, respectively. In the heating mode, the electricity rate required by the air source heat pump, $E^{SH}_{k_{ASHP},d,hr}$, to provide the heat rate, $H^{SH}_{k_{ASHP},d,hr}$, is formulated as:

$$E^{SH}_{k_{ASHP},d,hr} = H^{SH}_{k_{ASHP},d,hr}/COP^{SH}_{k_{ASHP}}, \quad \forall k_{ASHP}, \quad \forall d, hr, \tag{32}$$

where $COP^{SH}_{k_{ASHP}}$ is the coefficient of performance of the heat pump in the hating mode defined similarly as in Eq. (25).

Modeling of cooling mode is similar to that of heating described above.

*2.4.3.6. Energy storage devices.* For the operation of energy storage devices, the amount of energy stored at the beginning of each time interval equals the non-dissipated energy stored at the beginning of the previous time interval (based on the storage loss fraction), plus the net energy flow (energy input rate to the storage minus energy output rate from the storage) [2,34]. For the electrical energy storage, it can be expressed as:

$$E^{e,sto}_{ES,d,hr} = E^{e,sto}_{ES,d,hr-1}(1 - \varphi_{ES}(D_t)) + (E^{e,in}_{ES,d,hr} - E^{e,out}_{ES,d,hr})D_t, \quad \forall d, hr, \tag{33}$$

where $\varphi_{ES}(D_t)$ is the loss fraction, which takes into account the dissipated energy during the time interval, $D_t$.

Modeling of thermal storage systems for domestic hot water, and space heating and cooling is similar to that described above.

### 2.5. Optimization method

With the exergetic objective function formulated in Eq. (11) and the economic one formulated in Eq. (1), the problem has two objective functions to be minimized. To solve this multi-objective optimization problem, a single objective function is formulated as a weighted sum of the total annual cost, $C_{TOT}$, and the total annual primary exergy input, $Ex_{in}$, to be minimized:

$$F_{obj} = c\omega C_{TOT} + (1 - \omega)Ex_{in}, \tag{34}$$

where constant $c$ is a scaling factor, chosen such that $c\,C_{TOT}$ and $Ex_{in}$ have the same order of magnitude. The Pareto frontier is found by varying the weight $\omega$ in the interval 0–1. The solution that minimizes the total annual cost can be found when $\omega = 1$, whereas the one that minimizes the total annual primary exergy input (i.e., maximizes the overall exergy efficiency) can be found when $\omega = 0$. The problem formulated above is linear, and involves both discrete and continuous variables. Branch-and-cut, which is powerful for mixed-integer linear problems, is therefore used.

## 3. Numerical testing

The method developed in Section 2 is implemented by using IBM ILOG CPLEX Optimization Studio Version 12.6. A hypothetic cluster of 30 buildings of residential sector located in Turin (Italy) is chosen as the targeted end-user. The optimization is carried out on an hourly basis for a representative day per season to reduce the variables number and the model complexity [2,41,42].

In the following, the input data are described in Section 3.1. The Pareto frontier is presented in Section 3.2. The optimized DESs configurations obtained under the economic and exergetic optimization as well as under two representative trade-off points on the Pareto frontier are compared in Section 3.3. The operation strategies of the energy devices in the optimized DES configurations under the economic and exergetic optimization are presented in Section 3.4.

### 3.1. Input data

The required input data include energy demand of the building cluster, solar energy availability, prices and exergy factors of primary energy carriers, and technical and economic information of energy devices as presented in the following.

Please cite this article in press as: Di Somma M et al. Multi-objective design optimization of distributed energy systems through cost and exergy assessments. Appl Energy (2017), http://dx.doi.org/10.1016/j.apenergy.2017.03.105

*3.1.1. Energy demand of the building cluster*

Each building is assumed to have a surface area of 5000 $m^2$, and a shape factor S/V of 0.5 $m^{-1}$. The hourly energy rate demand for electricity, domestic hot water, space heating, and space cooling of the building cluster for four representative season days are built based on [56–58], as shown in Fig. 2. To compute the annual energy requirements of the building cluster, the year is assumed to include 90 days in the cold season (December – February), 92 days in the cold mid-season (October 15 – November 30, and March 1 – April 15), 91 days in the hot mid-season (April 15 – May 31, and September 1 – October 15), and 92 days in the hot season (June – August). This assumption is based on the climatic characteristics of the zone, and on the period established by the current Italian law when it is possible to turn on the heating systems in the relative climatic zone (from mid-October to mid-April). Table 1 shows the annual energy requirements of the building cluster.

*3.1.2. Solar energy availability*

Information about solar energy is taken from the meteorological data in Turin [59]. The hourly solar irradiance on a 35° tilted surface for each representative season day is evaluated as the average of the hourly mean values of the solar irradiance in the corresponding hour of all days in the relative season. The average hourly solar irradiance profiles for the four representative season days are shown in Fig. 3. The maximum available area for installation of solar collector and PV arrays is assumed as 5000 $m^2$.

*3.1.3. Prices and exergy factors of primary energy carriers*

Energy prices are chosen according to the Italian market. The unit price of grid power is assumed as 0.15 €/kW h, whereas the unit prices of natural gas and biomass (wood pellet) are assumed as 0.477 €/N $m^3$, and 120 €/ton, respectively. The exergy efficiency of power generation plants is assumed as 0.40, based on the fossil fuel energy mix for electricity production and on the average efficiency of fossil fuel-fired electricity production in Italy [60,61]. The exergy factors of natural gas and biomass are assumed as 1.04 and 1.16 [50], respectively. In the evaluation of the Carnot factor for the solar exergy input rate (Eq. (14)), the temperature of the heat transfer fluid at the exit of the collector field is assumed constant and equal to 353.15 K.

**Table 1**
Annual energy requirements of the building cluster (MW h).

| Season | Electricity | Domestic hot water | Space heating | Space cooling |
|---|---|---|---|---|
| Cold | 1114 | 544.3 | 6227 | 0 |
| Cold-mid | 1139 | 556.4 | 3378 | 0 |
| Hot-mid | 1126 | 550.3 | 0 | 0 |
| Hot | 1139 | 556.4 | 0 | 3235 |

*3.1.4. Technical and economic information of energy devices*

The technical and economic information of energy devices are summarized in Table 2, and they are based on a detailed market analysis [36–38,44,62–69]. For each energy device, Table 2 shows: the minimum and maximum sizes, specific capital costs, O&M costs, efficiencies and lifetime. For CHPs, specific capital costs, O&M costs as well as electrical and thermal efficiencies strongly vary with the sizes. For CHPs with gas-fired internal combustion engine and with micro-turbines, the entire size ranges available in the market are divided into several small ranges, respectively, while the characteristics assumed in each size range are shown in Fig. 4a and b [62,64,68]. Similarly, the capital cost of single-stage absorption chillers is also subject to economies of scale, and the specific capital cost assumed in each size range is shown in Fig. 5 [64,68]. Conversely, O&M costs and efficiencies are assumed constant and equal to the average values in the size range, due to the slight variation of these characteristics with sizes. For

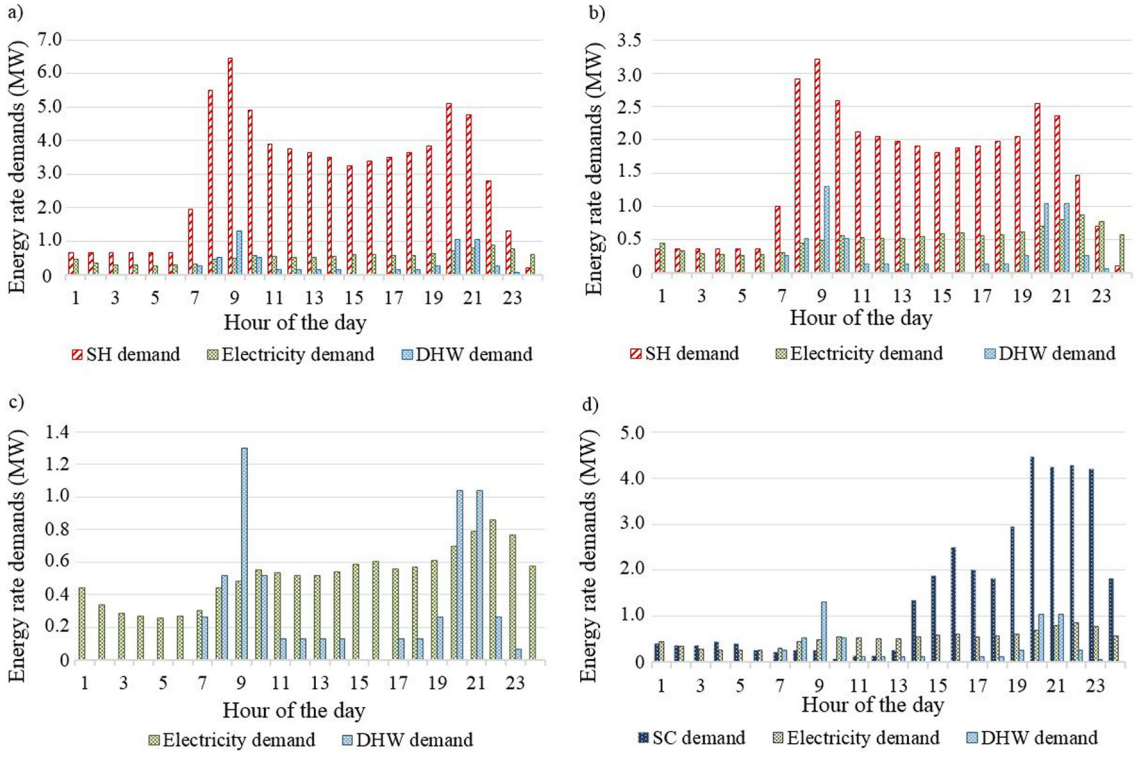


**Fig. 2.** Hourly mean energy rate demand of the hypothetic building cluster: (a) a representative cold season day; (b) a representative cold mid-season day; (c) a representative hot mid-season day; and (d) a representative hot season day.

Please cite this article in press as: Di Somma M et al. Multi-objective design optimization of distributed energy systems through cost and exergy assessments. Appl Energy (2017), http://dx.doi.org/10.1016/j.apenergy.2017.03.105

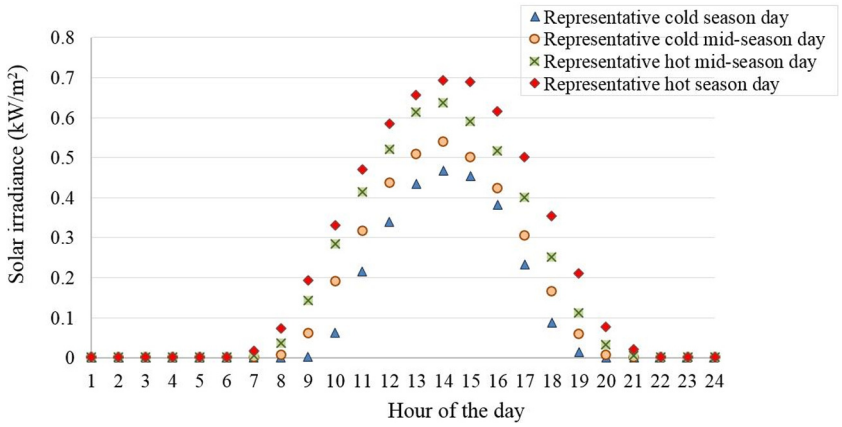


**Fig. 3.** Average hourly solar irradiance profiles for the four representative season days.

**Table 2**
Technical and economic information of energy devices.

| Energy device | Size range (kW) | Specific capital cost | O&M costs (€/kW h) | Efficiency | | Lifetime |
|---|---|---|---|---|---|---|
| | | | | Electrical | Thermal | |
| CHP NG ICE | 20–5000 | 840–1495 €/kW | 0.008–0.023 | 0.28–0.41 | 0.40–0.68 | 20 |
| CHP NG MTG | 30–300 | 1630–2492 €/kW | 0.011–0.019 | 0.26–0.32 | 0.44–0.52 | 20 |
| NG boiler | 10–2000 | 100 €/kW | 0.0014 | | 0.9 | 15 |
| Biomass boiler | 10–2000 | 400 €/kW | 0.0027 | | 0.85 | 15 |
| Solar PV | – | 2000 €/$kW_p$ | 0.010 | | 0.14 | 30 |
| Solar thermal | – | 200 €/$m^2$ | 0.0057 | | 0.6 | 15 |
| Air-source heat pump | 10–5000 | 460 €/kW | 0.0025 | | $COP^{SH}$ = 3.5<br>$COP^{SC}$ = 3.0 | 20 |
| Absorption chiller | 10–5000 | 230–510 €/kW | 0.0020 | | $COP$ = 0.8 | 20 |
| Electrical storage | – | 350 €/kW h | 0.005 | $\varphi_{ES}$ = 0.25 | | 5 |
| Thermal storage | – | 20 €/kW h | 0.0012 | | $\varphi_{TES}$ = 0.05 | 20 |

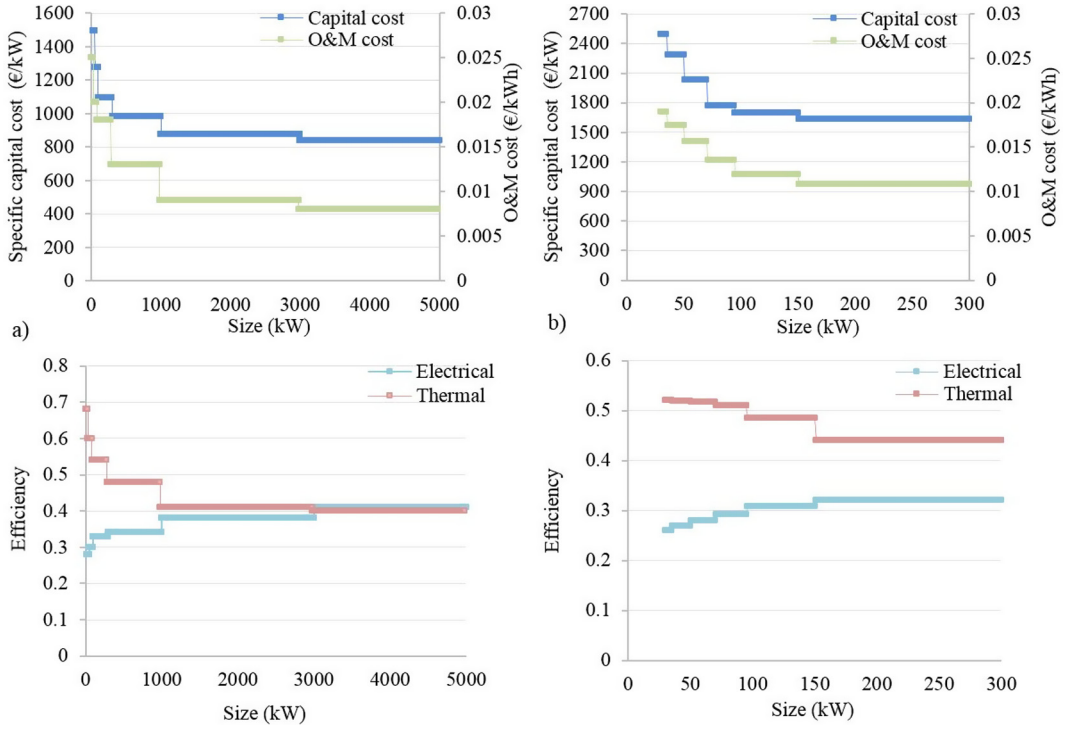


**Fig. 4.** Specific capitals costs and efficiencies vs. sizes of: (a) CHP with gas-fired internal combustion engine and (b) CHP with gas-fired micro-turbines.

Please cite this article in press as: Di Somma M et al. Multi-objective design optimization of distributed energy systems through cost and exergy assessments. Appl Energy (2017), http://dx.doi.org/10.1016/j.apenergy.2017.03.105

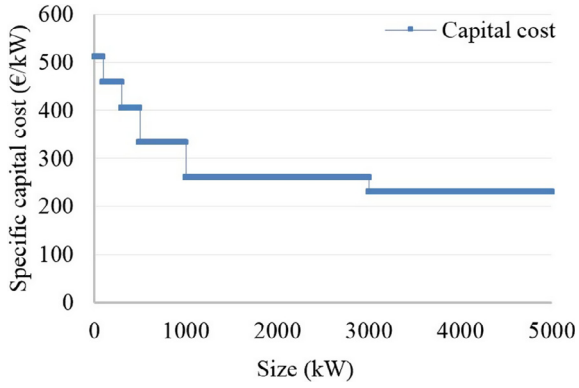


**Fig. 5.** Specific capital cost vs. size of single-stage absorption chillers.

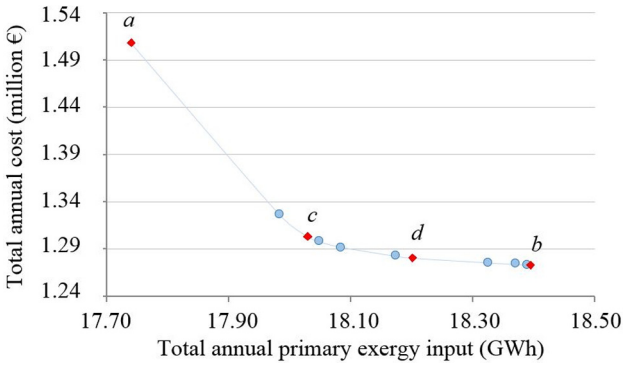


**Fig. 6.** Pareto frontier.

boilers and air-source heat pumps, the specific capital costs, O&M costs and efficiencies are assumed constant and equal to the average value in the size range considered, due to the slight variation of these characteristics with sizes [63,65–68]. Lead-acid batteries are assumed as electrical storage devices [38]. Moreover, the maximum number of energy devices associated to each technology is assumed as two. To evaluate the total annualized investment cost, the interest rate is assumed as 5%.

### 3.2. Pareto frontier

For the numerical testing, there are 50,552 constraints; 19,065 binary decision variables; 4,139 other decision variables; and 121,736 non-zero coefficients. The optimization problem can be solved within few hours with a mixed integer gap lower than 0.15% with a PC with 2.60 GHz (2 multi-core processors) Intel(R) Xeon(R) E5 CPU and 32G RAM. The Pareto frontier is shown in Fig. 6. The point marked with *a* is obtained under the exergetic optimization ($\omega = 0$), where the total annual cost is 1.508 MEuro and the total annual primary exergy input is 17.740 GW h. The point marked with *b* is obtained under the economic optimization ($\omega = 1$), where the total annual cost is 1.273 MEuro and the total annual primary exergy input is 18.394 GW h. The points between these two extreme points are found by subdividing the weight interval into 10 equally-spaced points. Each point on the Pareto frontier corresponds to a different optimized configuration of the DES, thereby providing different design options for planners based on short- and long-run priorities.

### 3.3. Optimized DES configurations

The optimized configurations of the DESs (numbers, sizes and total installed capacities of energy devices), and the economic and exergetic performances for points *a* and *b* on the Pareto frontier are shown in Table 3. For the illustration purpose, the points marked with *c* and *d* in Fig. 6 are chosen to show the optimized configuration of the DES under a higher weight of 0.8 for the exergetic objective ($\omega = 0.2$), and a higher weight of 0.6 for the economic objective ($\omega = 0.6$), respectively.

Under the exergetic optimization, the total capacity of CHPs with gas-fired internal combustion engine is the largest among

**Table 3**
Optimized solutions at points *a*, *b*, *c* and *d* on the Pareto Frontier.

| Optimized solutions | | Point *a* | Point *c* | Point *d* | Point *b* |
|---|---|---|---|---|---|
| CHP NG ICE | Number | 2 | 2 | 2 | 2 |
| | Sizes ($MW_{el}$) | 1.122–1.981 | 0.372–1.190 | 0.30–1.095 | 0.30–1.0 |
| | Total ($MW_{el}$) | 3.103 | 1.562 | 1.395 | 1.30 |
| CHP NG MTG | Number | 2 | 0 | 0 | 0 |
| | Sizes ($MW_{el}$) | 0.095–0.270 | – | – | – |
| | Total ($MW_{el}$) | 0.365 | – | – | – |
| NG boiler | Number | 0 | 0 | 1 | 2 |
| | Sizes ($MW_{th}$) | – | – | 0.538 | 0.261–0.696 |
| | Total ($MW_{th}$) | – | – | 0.538 | 0.957 |
| Biomass boiler | Number | 0 | 0 | 0 | 0 |
| | Sizes ($MW_{th}$) | – | – | – | – |
| | Total ($MW_{th}$) | – | – | – | – |
| Solar PV | Size ($MW_{el}$) | 0.446 | 0.452 | 0.485 | 0.485 |
| | Area ($m^2$) | 4593 | 4746 | 5000 | 5000 |
| Solar thermal | Size ($MW_{th}$) | 0.169 | 0.106 | – | – |
| | Area ($m^2$) | 407 | 254 | – | – |
| Air-source heat pump | Number | 2 | 2 | 2 | 2 |
| | Sizes ($MW_{th}$) | 2.120–3.0 | 0.721–3.0 | 0.268–2.925 | 0.269–2.595 |
| | Total ($MW_{th}$) | 5.120 | 3.721 | 3.193 | 2.864 |
| Absorption chiller | Number | 2 | 1 | 1 | 1 |
| | Sizes ($MW_{th}$) | 0.50–0.968 | 1.265 | 1.0 | 1.0 |
| | Total ($MW_{th}$) | 1.468 | 1.265 | 1.0 | 1.0 |
| Electrical storage | Total capacity ($MW\ h_{el}$) | 0 | 0 | 0 | 0 |
| DHW storage | Total capacity ($MW\ h_{th}$) | 1.062 | 1.670 | 1.906 | 2.093 |
| SH storage | Total capacity ($MW\ h_{th}$) | 1.60 | 1.315 | 1.585 | 1.425 |
| SC storage | Total capacity ($MW\ h_{th}$) | 0.182 | 0.485 | 1.233 | 1.976 |
| Total annual cost (million €) | | 1.508 | 1.303 | 1.280 | 1.273 |
| Total annual primary exergy input (GW h) | | 17.740 | 18.030 | 18.326 | 18.394 |

Please cite this article in press as: Di Somma M et al. Multi-objective design optimization of distributed energy systems through cost and exergy assessments. Appl Energy (2017), http://dx.doi.org/10.1016/j.apenergy.2017.03.105

the four configurations, and similarly for CHPs with gas-fired micro-turbine. This highlights the importance of CHPs for the exergetic objective, due to the possibility of waste heat recovery for thermal purposes, thereby promoting efficient use of the energy resource through a better exploitation of its potential. The large-size CHPs with gas-fired internal combustion engine are selected to satisfy the high electricity loads, whereas the small-size CHPs with micro-turbine are selected to satisfy the low electricity loads. As $\omega$ increases, only CHPs with internal combustion engines are selected instead of CHPs with micro-turbines, due to their higher total energy efficiency and lower investment and O&M costs. The chosen CHPs are one small and one large in order to cover most of the electricity load until their minimum part loads. However, the total capacity of CHPs with internal combustion engines reduces, reaching the minimum under the economic optimization, mostly due to the high investment cost. Conversely, the total capacity of natural gas boilers reaches the maximum under the economic optimization, due to the low investment and O&M costs, whereas they are not selected under the exergetic optimization and under a higher weight of the exergetic objective (at point *c*). This result clearly indicates that natural gas, as a high-quality energy resource, should not be used for low-quality thermal demand.

Biomass boilers are not selected in any configuration. The absence of biomass boilers under the exergetic optimization clearly shows that exergy analysis is a powerful tool for designing more sustainable energy supply systems, showing that biomass as a high-quality renewable energy resource, should not be used for low quality thermal demand. Biomass could be used instead for meeting high exergy demand such as for electricity generation, with a better exploitation of the potential of the fuel. In DES design optimization, minimization of not only fossil but also renewable exergy input promotes efficient use of all energy resources, while highlighting that even renewable energy sources need to be used efficiently based on their potential. This result agrees with those presented in [34], where in the operation optimization of a DES, biomass boilers were not used under the exergetic optimization, but they were used under the energy cost minimization due to the low price of biomass. Moreover, this result also agrees with those presented in [16], where different energy systems (i.e., gas-fired boiler, biomass boiler, ground-source heat pump, and waste district heat) were compared through exergy analysis to meet thermal demand in buildings. It was shown that exergy input of the biomass boilers is the largest among the four options, since biomass, although renewable, is a high-quality energy resource, thereby resulting to be not convenient to meet low-quality thermal demand. As for DES design optimization, also under the economic optimization, biomass boilers are not selected due to the high investment cost.

As for solar energy systems, the entire available area is occupied in all the optimized configurations. Under the economic optimization, the entire area is occupied by PV arrays, highlighting the convenience of this technology for the economic objective, especially thanks to the current low costs. The size of PV arrays decreases as $\omega$ decreases, reaching the minimum under the exergetic optimization, since the available area is also occupied by solar thermal collectors, whose area is equal to 0 under the economic optimization, and reaches the maximum under the exergetic optimization. This result highlights the convenience of solar thermal for the exergetic purpose, due to the low exergy related to the thermal energy output from the collectors, used to meet the low-quality thermal demand.

The total capacities of air-source heat pumps and absorption chillers increase as $\omega$ decreases, reaching the maximum under the exergetic optimization, highlighting their convenience for the exergetic purpose, due to the high conversion efficiency and the possibility of waste heat recovery for space cooling demand, respectively. When $\omega$ increases, their total capacities reduce, thereby reducing the total annual cost. Electrical storage (i.e., lead–acid battery) is never selected. The high investment cost makes this technology not competitive. Therefore, it is not selected under the economic optimization. Under the exergetic optimization, electrical storage is not selected mostly due to the high storage loss fraction. As for thermal storage for space cooling demand, the capacity strongly increases as the weight for the economic objective increases, reaching the maximum under the economic optimization. This result clearly shows the economic convenience of the thermal storage for the space cooling demand, whose capacity is strongly related to the sizing of absorption chillers. With larger storage capacity, smaller size of absorption chillers are needed, and the total investment cost reduces.

The capacity of thermal storage for domestic hot water demand is maximum under the economic optimization. The capacity of thermal storage for space heating demand slightly changes with the weight and is maximum under the exergetic optimization. Differently from the thermal storage for space cooling, whose capacity is strongly related to the sizing of absorption chillers, the capacities of thermal storage for domestic hot water and space heating demand mostly depend on the amount of exhaust gas recovered by CHPs, and therefore depend on the operation strategies of multiple energy devices to be discussed later.

The total annual cost and primary exergy input are also investigated for a conventional energy supply system, where grid power is used for the electricity demand, gas-fired boilers for domestic hot water and space heating demand, and electric chillers fed by grid power for space cooling demand. The total annual cost is equal to 1.914 MEuro, and the total annual primary exergy input is equal to 27.641 GW h. Fig. 7 shows the reduction in total annual cost and primary exergy input of the DES configurations at points *a*, *b*, *c* and *d* on the Pareto frontier, as compared with the conventional energy supply system. The maximum reduction in total annual cost, equal to 33.5%, is attained under the economic optimization, whereas the reduction in the total annual primary exergy input is the minimum one, equal to 33.5%. Conversely, the maximum reduction in total annual primary exergy input, equal to 35.8%, is attained under the exergetic optimization, whereas the reduction in total annual cost is the minimum one, equal to 21.2%. Therefore, in all the optimized DES configurations, strong reduction in total annual cost and primary exergy input is attained as compared with the conventional energy supply system.

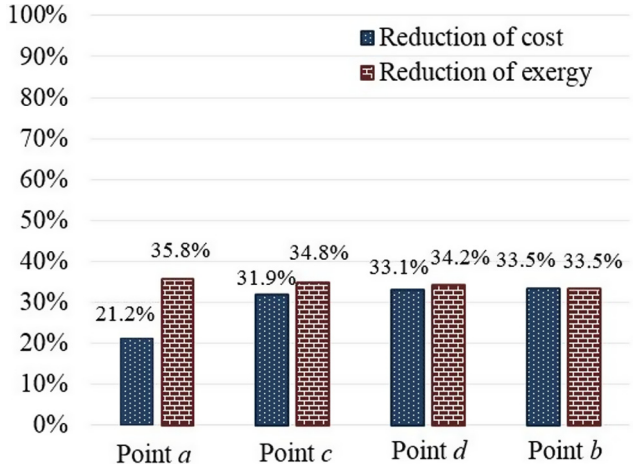


**Fig. 7.** Reduction in total annual cost and primary exergy input of the optimized DES configurations at points *a*, *b*, *c* and *d* on the Pareto frontier, as compared with the conventional energy supply system.

Please cite this article in press as: Di Somma M et al. Multi-objective design optimization of distributed energy systems through cost and exergy assessments. Appl Energy (2017), http://dx.doi.org/10.1016/j.apenergy.2017.03.105

### 3.4. Operation strategies of energy devices in the optimized DES configurations under economic and exergetic optimization

For different optimized DES configurations, different operation strategies of energy devices are found. For the illustration purpose, the operation strategies of the energy devices in the optimized DES configurations obtained under the exergetic and economic optimization in the four representative season days are compared in Fig. 8.

Fig. 8a for electricity, shows the total grid power, and the total electricity provided by CHPs and PV to meet the load as the sum of the total demand and the total electricity required by air-source heat pumps in the four representative season days. Under both exergetic and economic optimization, electricity from power grid is generally lower than the electricity provided by CHPs, highlighting that CHP is convenient for both objectives. Moreover, CHPs with micro-turbines are used only under the exergetic optimization, since they are not selected under the economic optimization as presented in the previous subsection, and the electricity provided is smaller than that provided by CHPs with internal combustion engines, coherently with the larger size of the latter CHPs. In the hot mid-season day, the total electricity provided by CHPs is lower than in the other days under both the exergetic and economic optimization, since only electricity and domestic hot water demand need to be satisfied in this day. In this day, under the exergetic optimization, the electricity from power grid is larger than in the other days, and it is also larger than the total electricity provided by CHPs, due to the contribution of solar thermal to meet the domestic hot water demand, as shown in Fig. 8b. It can be also noted that the electricity provided by PV is slightly larger under the economic optimization than under the exergetic one, coherently with the larger size of PV attained under the economic optimization as discussed in the previous subsection.

Fig. 8b for domestic hot water demand shows the total thermal energy provided by CHPs, gas-fired boilers, solar thermal collectors, as well as the total thermal energy input and output to/from the storage to meet the total demand in the four representative season days. Under the economic optimization, the thermal energy from exhaust gas is larger than under the exergetic one. This is due to the fact that, in absence of solar thermal, a larger amount of exhaust gas is used to meet the demand as compared to the exergetic optimization. Natural gas boilers are only used under the economic optimization, since they are not selected under the exergetic optimization as presented in the previous subsection. As for thermal storage, it is generally more used under the economic optimization than under the exergetic one, due to the larger amount of exhaust gas, which also explains the larger capacity required under the economic optimization.

Fig. 8c for space heating and cooling demand shows the total thermal energy provided by CHPs, gas-fired boilers, air-source heat pumps, absorption chillers as well as the total thermal energy input and output to/from the storage systems to meet the total

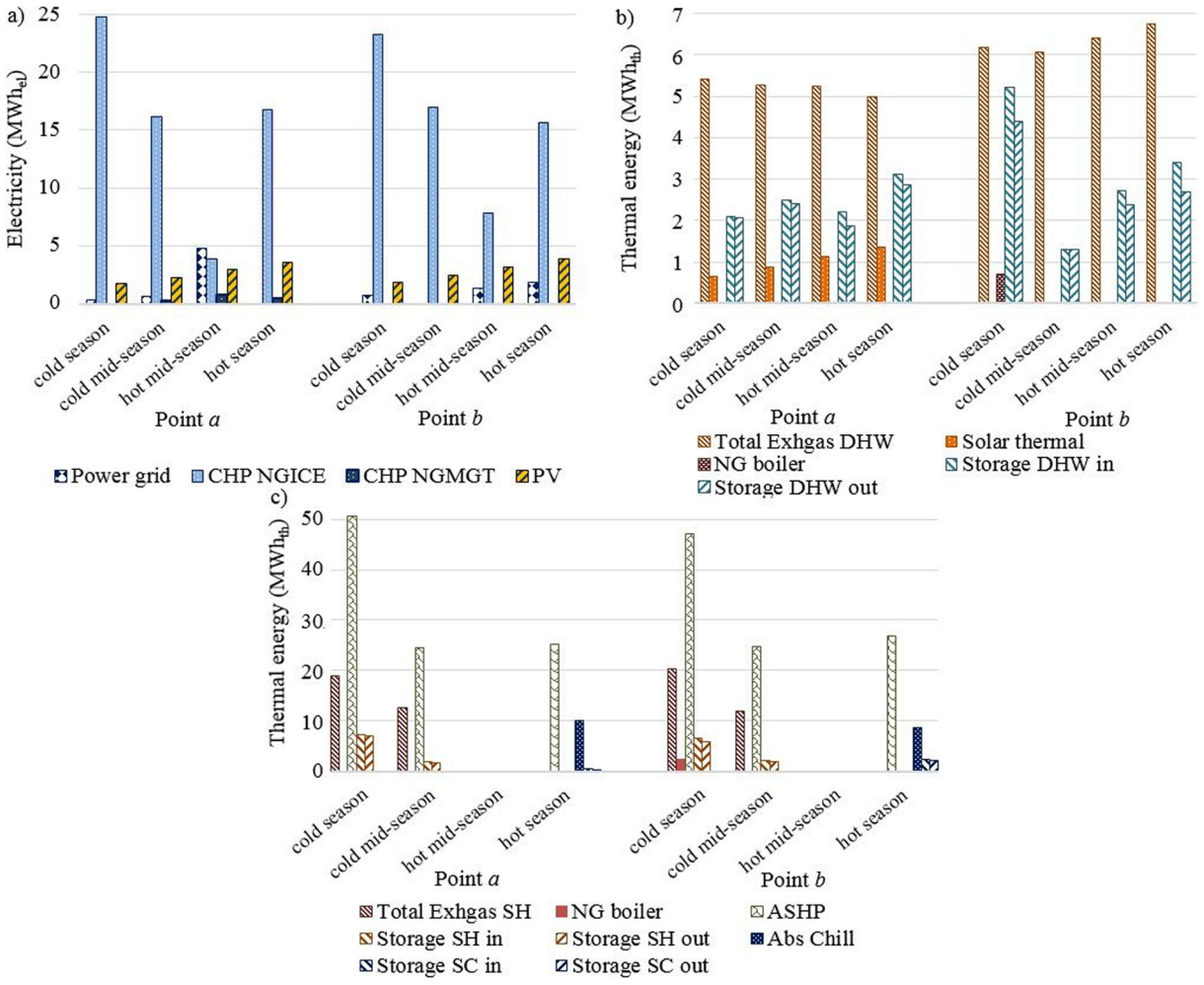


**Fig. 8.** Operation strategies of optimized DES configurations at points *a* and *b* in the four season days for (a) electricity; (b) domestic hot water; and (c) space heating and cooling.

Please cite this article in press as: Di Somma M et al. Multi-objective design optimization of distributed energy systems through cost and exergy assessments. Appl Energy (2017), http://dx.doi.org/10.1016/j.apenergy.2017.03.105

demands in the four representative season days. For space heating, heat pumps are mostly used to meet the demand under both exergetic and economic optimization, highlighting that this technology is convenient for both the objectives. Heat pumps are generally more used under the exergetic optimization than under the economic one. Similarly to the case of domestic hot water demand, natural gas boilers are only used under the economic optimization. As for thermal storage, the slightly larger capacity required under the exergetic optimization than under the economic one is due to the fact that with a larger usage of heat pumps to meet the demand, a larger amount of exhaust gas is dispatched to charge the storage, as compared with what occurs under the economic optimization. For space cooling demand, similar to space heating demand, heat pumps are mostly used to meet the demand under both exergetic and economic optimization. The thermal energy provided by the absorption chillers is larger under the exergetic optimization than under the economic one, coherently with the larger size attained under the exergetic optimization as presented in the previous subsection. As for thermal storage, it is much more used under the economic optimization than under the exergetic one, in accordance to the larger capacity required under the economic optimization.

## 4. Sensitivity analysis

A sensitivity analysis is carried out to investigate the influence of key parameters such as energy prices and energy demand scale on the optimized DES configurations and the related economic and exergetic performances. In the following, the results of the sensitivity analysis on energy prices and energy demand scale are presented and discussed in s 4.1 and 4.2, respectively.

### 4.1. Energy price sensitivity

The operation strategies of energy devices strongly depend on energy prices, which in turn affect their combination and sizes in the DES configurations attained by the optimization model. With the increasing consumption of energy resources, energy prices are expected to increase in next years. In the multi-objective optimization problem, the effect of the energy price increase is maximum under the economic optimization, while no effects are under the exergetic optimization. Results of the economic optimization carried out by considering the increase of electricity and natural gas price are presented and discussed in the following. As for biomass, the effect of the price increase is not investigated, since even with the current price, biomass boilers are not selected under the economic optimization.

#### 4.1.1. Electricity price sensitivity under the economic optimization

The results obtained for electricity price increases of 25% until 100% of the current value are compared in Fig. 9. Fig. 9a shows the increase in the total annual cost and primary exergy input as compared with those obtained with the current electricity price. It can be noted that the economic performance are more affected by the electricity price increase than the exergetic ones. However, the effect of electricity price increase on the economic performance is not that significant: when the electricity price is twice of the current one, the increase in the total annual cost is less than 2%. This is due to the fact that, even with the current electricity price, electricity from the power grid is much less than that provided by CHPs as discussed in the previous section.

For the illustration purpose, the total installed capacities of energy devices in the optimized DES configurations obtained with 50% and 100% electricity price increase and those obtained with the current electricity price are compared in Fig. 9b. As the electricity price increases, the total installed capacity of CHP with gas-fired internal combustion engine increases, since CHPs become more convenient. Similar to the current electricity price, also with higher electricity prices, CHPs with gas- fired micro-turbine are not chosen, due to the high investment costs. When electricity price increases, the size of PV systems reduces, due to the larger capacity of CHPs used to meet the electricity load. Solar thermal is not selected as occurs with the current electricity price. The total capacity of air-source heat pumps and gas-fired boilers remains almost unchanged. However, the total capacity of heat pumps reaches the maximum when the electricity price is twice of the current one due to their high conversion efficiencies, whereas the contrary occurs for gas-fired boilers. With larger usage of heat pumps, boilers are less used to meet the space heating demand. Biomass boilers are not selected due to the high investment costs. As for absorption chillers, the total capacity reaches the maximum when the electricity price is twice of the current one, mainly due to the larger usage of CHPs and consequent larger amount of exhaust gas used for the space cooling demand. This latter also explains the significant increase of the capacity of storage for the space cooling demand occurring when the electricity price increases.

The effect of electricity price increase on the exergetic performances is negligible. However, the small increase in the total annual primary exergy input occurring for higher electricity prices is due to the reduction in the usage of PV systems and the consequent larger usage of natural gas in CHPs to meet the electricity load. This result highlights the importance of PV systems for the exergetic purpose, since the usage of electricity from PV systems to meet high-quality electricity demand results to be better than burning natural gas.

#### 4.1.2. Natural gas price sensitivity under the economic optimization

For natural gas price increases of 25% until 100% of the current value, the results are compared in Fig. 10. Fig. 10a shows the increase in the total annual cost and primary exergy input as compared with those obtained with the current natural gas price. It can be noted that the natural gas price increase has larger effects on both the economic and exergetic performances than electricity price increase: when the natural gas price is twice of the current one, the increase in the total annual cost and primary exergy input are equal to 22.6% and 33.5%, respectively. With the current price, natural gas is the most used primary energy carrier, since it is used to feed both CHPs and gas-fired boilers, which are much used under the economic optimization, as discussed in the previous section. Therefore, the effect of natural gas increase on the economic and exergetic performances becomes significant.

The total installed capacities of energy devices in the optimized DES configurations obtained with 50% and 100% natural gas price increase and those obtained with the current natural gas price are compared in Fig. 10b. As the natural gas price increases, the total installed capacity of CHP with gas-fired internal combustion engine dramatically reduces, reaching the minimum when the gas price is twice of the current one, whereas CHPs with gas-fired micro-turbine are not selected as occurs with the current natural gas price. The total installed capacity of gas-fired boilers reduces as the gas price increases, even though the reduction of the total capacity is not such significant as that of CHPs. This is because when natural gas price increases, grid power becomes much more convenient than CHPs to meet the electricity load, due to the high investment costs. The increase of natural gas price has a lower impact on the installed capacity of gas-fired boilers. Although the gas price increase, gas-fired boilers have low investment costs, and they are still convenient for the economic objective. When natural gas price increases, biomass boilers become more convenient than gas-fired boilers, and they are selected in the optimized DESs configurations, although their investment

Please cite this article in press as: Di Somma M et al. Multi-objective design optimization of distributed energy systems through cost and exergy assessments. Appl Energy (2017), http://dx.doi.org/10.1016/j.apenergy.2017.03.105

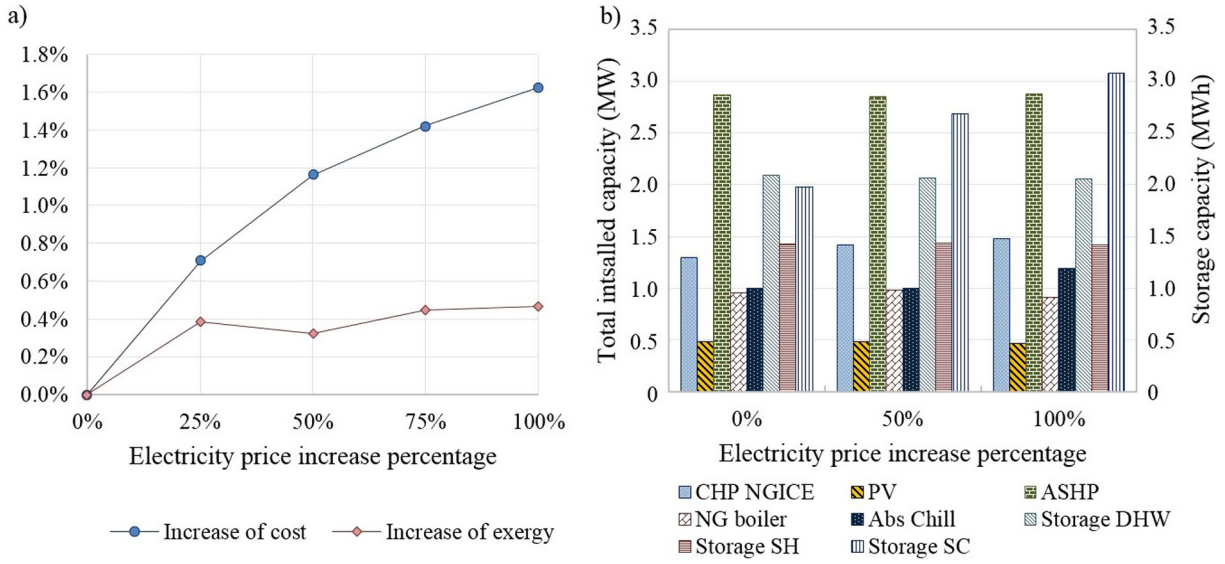


**Fig. 9.** (a) Economic and exergetic performance of optimized DES configurations under the economic optimization for electricity price increases of 25% until 100% of the current value. (b) Total installed capacity of energy devices for various electricity price increases.

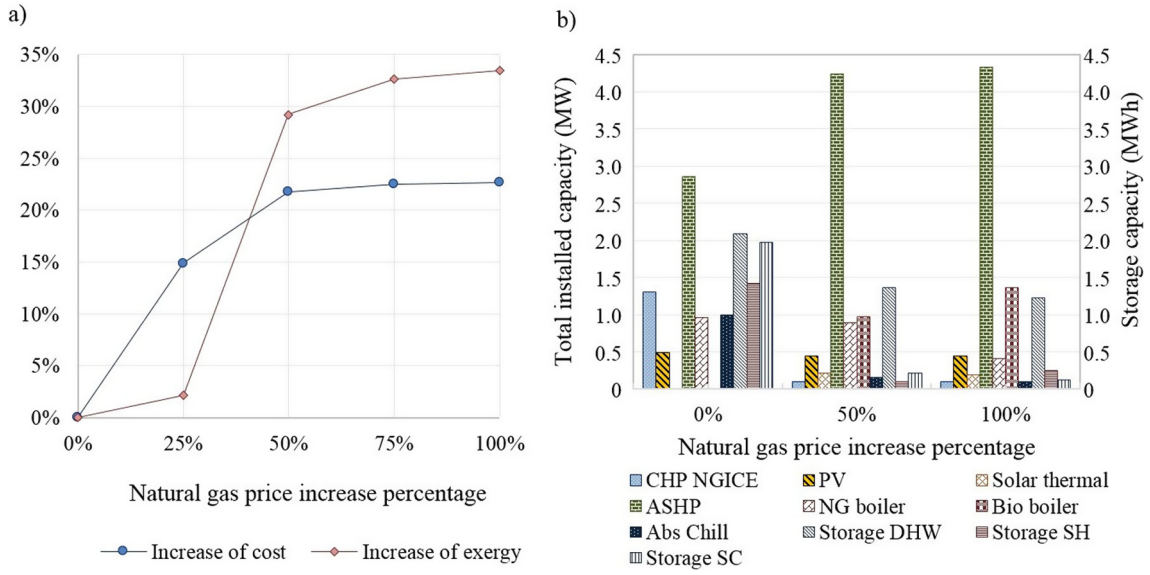


**Fig. 10.** (a) Economic and exergetic performance of optimized DES configurations under the economic optimization for natural gas price increases of 25% until 100% of the current value. (b) Total installed capacity of energy devices for various natural gas price increases.

costs are higher. For higher natural gas prices, the size of PV systems reduces, since the available area for installation of solar systems is also occupied by solar thermal collectors used to meet the demand of domestic hot water. As for air-source heat pumps, their installed capacity significantly increases when natural gas price increases, due to the strong reduction of exhaust gas from CHPs to meet the demand of space heating and cooling. This latter also explains the significant reduction of the total installed capacity of absorption chillers and of the required capacity of the storage for space cooling demand. The reduction of exhaust gas from CHPs under higher natural gas prices also explains the reduced required capacities of storage for domestic hot water and space heating demands. Similar to the current natural gas price, electrical storage is not selected due to the high investment costs.

The strong reduction in the usage of CHPs is one of the most important factors influencing the strong increase in the total annual primary exergy input occurring for natural gas price increases higher than 25% of the current value. This result underlines the importance of waste heat recovery from CHPs for the exergetic perspective, since, in absence of exhaust gas, other combustion-based energy devices are used to meet the thermal demand, thereby increasing the waste of high-quality energy. Another important factor influencing the increase in the total annual primary exergy is the usage of biomass boilers used to meet the thermal demand. As discussed earlier, biomass is a high-quality renewable energy resource, and it should not be used to meet low-quality thermal demand.

### 4.2. Energy demand scale sensitivity

The types, number and sizes of energy devices in the DES configurations strongly depend on energy demand, which is one of the uncertainty factors at the demand side. In the multi-objective optimization problem, the effect of energy demand variation is

Please cite this article in press as: Di Somma M et al. Multi-objective design optimization of distributed energy systems through cost and exergy assessments. Appl Energy (2017), http://dx.doi.org/10.1016/j.apenergy.2017.03.105

observable at all the points of the Pareto frontier. For the illustration purpose, the effect of energy demand variation (both electricity and thermal) is investigated under the economic and exergetic optimization in the following.

*4.2.1. Energy demand scale sensitivity under the economic optimization*

The results obtained under the economic optimization for energy demand decrease and increase of 25% until 50% of the current one, respectively, are compared in Fig. 11. According to Fig. 11a, both the total annual cost and primary exergy input vary almost linearly with the energy demand variation. For energy demand increase of 50% of the current one, the increase in total annual cost and primary exergy input reaches the maximum, equal to 50.0% and 53.5%, respectively. For energy demand decrease of 50% of the current value, the reduction in total annual cost and primary exergy input reaches the maximum, equal to 48.8% and 50.4%, respectively.

For the illustration purpose, the total installed capacities of energy devices in the optimized DES configurations obtained with 50% energy demand decrease and 50% energy demand increase are compared with those obtained with the current energy demand in Fig. 11b. As the energy demand increases, the total installed capacities of most of the energy devices increase. The size of PV systems remains unchanged, occupying the entire available area. CHPs with gas-fired micro-turbine are not selected in the optimized DES configurations, as occurs with the current energy demand. As for thermal storage, the total capacities increase as the energy demand increases, due to the larger amount of exhaust gas from CHPs dispatched to the storage devices. Similar to the current energy demand, the electrical storage is not selected due to the high investment costs. The increase in the total annual primary exergy input is mostly due to the larger usage of grid power to meet the electricity load, and the larger usage of gas-fired boilers to meet the thermal demand.

As the energy demand decreases, the total installed capacities of most of the energy devices decrease. Differently to the case of energy demand increase, the size of PV systems also decreases, and solar thermal is selected for the demand of domestic hot water. The area occupied by solar energy systems is equal to 3464 $m^2$, lower than the available one. As for thermal storage, the total capacities reduce as the energy demand reduces, due to the lower amount of exhaust gas from CHPs dispatched to the storage devices. The decrease in the total annual primary exergy input is mostly due to the lower usage of grid power to meet the electricity load, and the lower usage of gas-fired boilers to meet the thermal demand.

Under the economic optimization, CHPs with gas-fired internal combustion engine, gas-fired boilers and air-source heat pumps are the energy devices which are most influenced by the energy demand variation. When the energy demand is 50% higher than the current one, the total capacities of CHPs, boilers and heat pumps increase by 53.8%, 69.4%, and 55.9%, as compared to those obtained with the current energy demand, respectively. Conversely, when the energy demand is 50% lower than the current one, their total capacities decrease by 53.8%, 58.9%, and 54.7%, respectively. The variation of energy demand has also noticeable effects on the capacities of storage for domestic hot water and space cooling demand. When the energy demand is 50% higher than the current one, the capacities of storage for domestic hot water and space cooling increase by 56.7% and 86.7%, respectively, whereas for energy demand decrease of 50% than the current one, they reduce by 65.4% and 19.3%, respectively.

*4.2.2. Energy demand scale sensitivity under the exergetic optimization*

The results obtained under the exergetic optimization for energy demand decrease and increase of 25% until 50% of the current one, respectively, are compared in Fig. 12. Fig. 12a shows the reduction/increase in the total annual cost and primary exergy input as compared with those obtained with the current energy demand. Similar to what occurs under the economic optimization, both the total annual cost and primary exergy input vary almost linearly with the energy demand variation. For energy demand increase of 50% of the current one, the increase in total annual cost and primary exergy input reaches the maximum, equal to 42.5% and 51.2%, respectively. For energy demand decrease of 50% of the current value, the reduction in total annual cost and primary exergy input reaches the maximum, equal to 43.0% and 51.7%, respectively.

The total installed capacities of energy devices in the optimized DES configurations obtained with 50% energy demand decrease

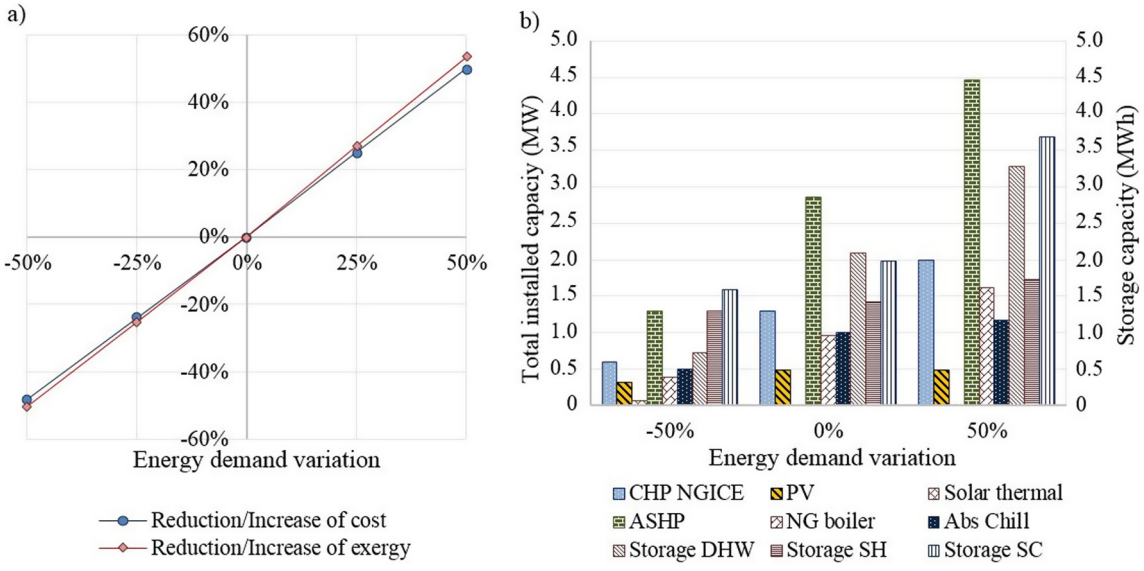


**Fig. 11.** (a) Economic and exergetic performance of optimized DES configurations under the economic optimization for energy demand decrease and increase of 25% until 50% of the current one, respectively. (b) Total installed capacity of energy devices for various energy demand decreases/increases.

Please cite this article in press as: Di Somma M et al. Multi-objective design optimization of distributed energy systems through cost and exergy assessments. Appl Energy (2017), http://dx.doi.org/10.1016/j.apenergy.2017.03.105

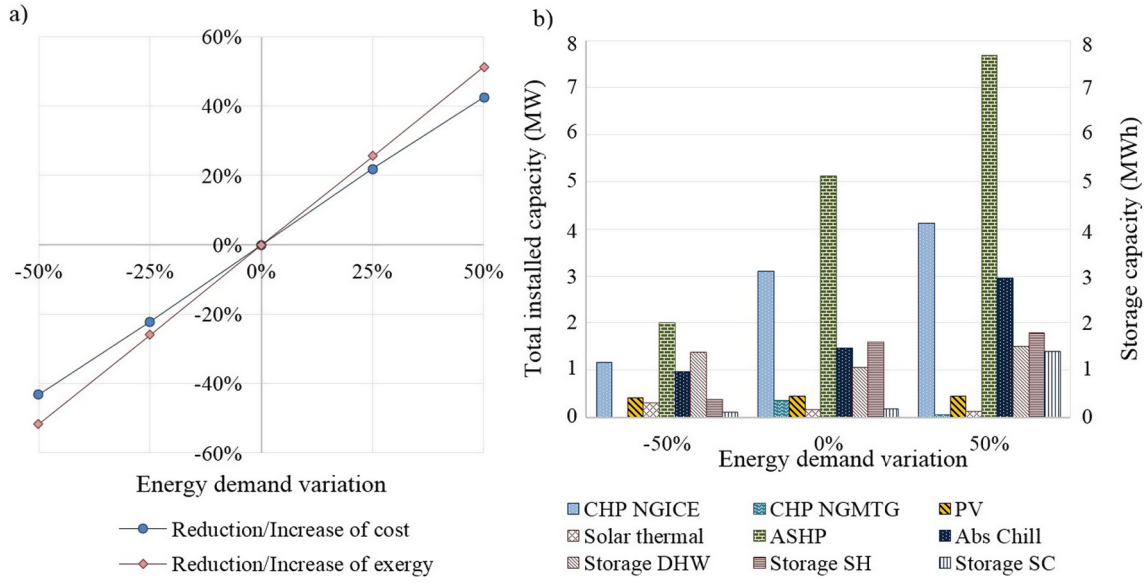


**Fig. 12.** (a) Economic and exergetic performance of optimized DES configurations under the exergetic optimization for energy demand decrease and increase of 25% until 50% of the current one, respectively. (b) Total installed capacity of energy devices for various energy demand decreases/increases.

and 50% energy demand increase are compared with those obtained with the current energy demand in Fig. 12b. As the energy demand increases, the total installed capacities of most of the energy devices increase. The opposite occurs for CHPs with gas-fired micro-turbine. The choice of only one CHP with gas-fired micro-turbine of 53 kW is related to the sizes of CHPs with gas-fired internal combustion engines, which are equal to 1.152 MW and 2.978 MW, instead of 1.122 MW and 1.981 MW attained with the current energy demand. Although the total capacity increases by 33.1% as compared to that obtained with the current energy demand, the size of the smaller CHP only increases by 2.7%. Therefore, these two CHPs, with the increase of electricity demand and the electricity required by heat pumps, can satisfy most of the total electricity load until their minimum part loads. The size of solar thermal also reduces as the energy demand increases, due the increase of the PV size, which occupy a larger area. As for thermal storage, the total capacities increase as the energy demand increases, due to the larger amount of exhaust gas from CHPs dispatched to the storage devices. The increase in the total annual cost is mostly due to larger investment costs related to the larger sizes of CHPs, air-source heat pumps and absorption chillers.

As the energy demand decreases, the total installed capacities of most of the energy devices decrease. For energy demand decrease of 50% than the current one, CHPs with gas-fired micro-turbine are not selected. This is related to the sizes of CHPs with gas-fired internal combustion engines, which are equal to 0.227 MW and 0.937 MW. The size of the smaller CHP decreases by 79.8% as compared to the smaller one in the current case. Therefore, the two CHPs can satisfy most of the total electricity load until their minimum part loads. Differently from the case of energy demand increase, the size of PV systems decreases, whereas the size of solar thermal increases. However, in all the optimized DES configurations, the entire available area for solar energy systems is occupied. As the energy demand decreases, the total capacities of storage for space heating and cooling reduce, due to the lower amount of exhaust gas from CHPs dispatched to the storage devices. As for thermal storage for domestic hot water, the total capacity increases, due to the larger amount of thermal energy from solar thermal dispatched to the storage. The reduction in the total annual cost is mostly due to lower investment costs related to the lower sizes of CHPs, air-source heat pumps and absorption chillers.

Under the exergetic optimization, CHPs with gas-fired internal combustion engine and with micro-turbine, air-source heat pumps, and absorption chillers are the energy devices which are most influenced by the energy demand variation. When the energy demand is 50% higher than the current one, the total capacities of CHPs with gas-fired internal combustion engine, heat pumps, and absorption chillers increase by 33.1%, 50.0%, and 100.0%, as compared to the those attained with the current energy demand, respectively. The total capacity of CHPs with micro-turbine reduces by 85.5%. Conversely, when the energy demand is 50% lower than the current one, their total capacities decrease by 62.5%, 60.7%, and 34.3%, respectively, and CHPs with micro-turbine are not selected. The variation of energy demand has also noticeable effects on the size of solar thermal, which reduces by 21.6% for energy demand increase of 50%, and increases by 82.1% for energy demand decrease of 50%. Remarkable effects of energy demand variation can be also noted on the capacities of storage for space heating and cooling demand.

## 5. Conclusions

In this paper, exergy is investigated in design optimization of distributed energy systems (DESs) for sustainable development of energy supply systems through multi-objective approach for not neglecting the crucial economic factor. Based on a pre-established DES superstructure with multiple energy devices such as combined heat and power and PV, a multi-objective linear programming problem is formulated to determine types, numbers and sizes of energy devices in the DES with the corresponding operation strategies in order to reduce the total annual cost and increase the overall exergy efficiency. In modeling of energy devices, the entire size ranges available in the market as well as the variations of efficiencies, specific capital and operation and maintenance costs with sizes are taken into account. The Pareto frontier is found by minimizing a weighted sum of the total annual cost and primary exergy input. The problem is solved by branch-and-cut. The

Please cite this article in press as: Di Somma M et al. Multi-objective design optimization of distributed energy systems through cost and exergy assessments. Appl Energy (2017), http://dx.doi.org/10.1016/j.apenergy.2017.03.105

models and methods provided can be applied in real contexts. Given the needed input data, the model allows to obtain the optimized combination of the candidate energy devices and the corresponding operation strategies through cost and exergy assessments, thereby providing decision support to planners.

Numerical results demonstrate that exergy analysis is a powerful tool for designing more sustainable energy supply systems based on the use of renewables and low-temperature sources for thermal demand in buildings, and on a better exploitation of the high potential of fossil fuels. Moreover, the Pareto frontier provides good balancing solutions for planners based on economic and sustainability priorities. It is found that, through proper design optimization, DESs can offer a good investment opportunity when compared with conventional energy supply systems, through rational use of energy resources. The total annual cost and primary exergy input of DESs with optimized configurations are significantly reduced as compared with a conventional energy supply system, where grid power is used for the electricity demand, gas-fired boilers for domestic hot water and space heating demand, and electric chillers fed by grid power for space cooling demand. As compared with the conventional case, the maximum reduction in the total annual cost and primary exergy input are equal to 33.5% and 35.8%, respectively. Also in the other points of the Pareto frontier, a strong reduction in total annual cost and primary exergy input is attained. In addition, a sensitivity analysis is carried out to analyze the influence of key parameters, such as energy prices and energy demand variation on the optimized DES configurations and the related economic and exergetic performances. It is found that natural gas price increase has larger effects than the electricity price increase on the optimized DES configurations and economic and exergetic performances, whereas the effects of energy demand variation are noticeable under both the economic and the exergetic optimization. The results found in this work clearly indicate that, among the candidate energy devices, combined heat and power systems with gas-fired internal combustion engine are the best options for both reduction of cost and primary exergy input, whereas solar energy systems are important for the exergetic purpose.

Although there are no exergy requirements as a methodology or an indicator yet in current energy legislations, results underline that exergy assessments may allow to meet the main goal of energy legislations in improving sustainability of energy supply. Minimization of not only fossil but also renewable exergy input promotes an efficient energy resource use through the reduction of the waste of high-quality energy, by avoiding burning processes and substituting them by low-temperature sources for thermal demand in buildings.

## References

[1] Kari A, Arto S. Distributed energy generation and sustainable development. Renew Sustain Energy Rev 2006;10:539–58.
[2] Ren H, Gao W. A MILP model for integrated plan and evaluation of distributed energy systems. Appl Energy 2010;87(3):1001–14.
[3] Akorede MF, Hizam H, Poresmaeil E. Distributed energy resources and benefits to the environment. Renew Sustain Energy Rev 2010;14:724–34.
[4] Pepermans G, Driesen J, Haesoldoncklx D, Belmans R, D'haeseleer W. Distributed generation: definition, benefits and issues. Energy Policy 2005;33:787–98.
[5] Söderman J, Pettersson F. Structural and operational optimisation of distributed energy systems. Appl Therm Eng 2006;26:1400–8.
[6] Bayod-Rujula AA. Future development of the electricity systems with distributed generation. Energy 2009;34(3):377–83.
[7] Huang J, Jiang C, Xu R. A review on distributed energy resources and microgrid. Renew Sustain Energy Rev 2008;12(9):2472–83.
[8] Han J, Ouyang L, Xu Y, Zeng R, Kang S, Zhang G. Current status of distributed energy system in China. Renew Sustain Energy Rev 2016;55:288–97.
[9] Chinese D, Meneghetti A. Optimisation models for decision support in the development of biomass-based industrial district-heating networks in Italy. Appl Energy 2005;82(3):228–54.
[10] Manfren M, Caputo P, Costa G. Paradigm shift in urban energy systems through distributed generation: methods and models. Appl Energy 2011;88(4):1032–48.
[11] Ruan Y, Liu Q, Zhou W, Firestone R, Gao W, Watanabe T. Optimal option of distributed generation technologies for various commercial buildings. Appl Energy 2009;86(9):1641–53.
[12] Ren H, Zhou W, Nakagami KI, Gao W, Wu Q. Multi-objective optimization for the operation of distributed energy systems considering economic and environmental aspects. Appl Energy 2010;87(12):3642–51.
[13] Pohekar SD, Ramachandran M. Application of multi-criteria decision making to sustainable energy planning—a review. Renew Sustain Energy Rev 2004;8(4):365–81.
[14] Wang JJ, Jing YY, Zhang CF, Zhao JH. Review on multi-criteria decision analysis aid in sustainable energy decision-making. Renew Sustain Energy Rev 2009;13(9):2263–78.
[15] Alarcon-Rodriguez A, Ault G, Galloway G. Multi-objective planning of distributed energy resources: a review of the state-of-the-art. Renew Sustain Energy Rev 2010;14:1353–66.
[16] ECBCS – Annex 49 – Low Exergy Systems for High Performance Buildings and Communities, homepage. Available <http://www.ecbcs.org/annexes/annex49.htm>.
[17] Dincer I, Rosen MA. Energy, environment and sustainable development. Appl Energy 1999;64(1):427–40.
[18] Dincer I, Rosen MA. Exergy-energy, environment and sustainable development. 1st ed. Oxford, UK: Elsevier Publication; 2007.
[19] Dincer I, Rosen MA. Exergy: energy, environment and sustainable development. Newnes; 2012.
[20] Wall G, Gong M. On exergy and sustainable development—part 1: conditions and concepts. Exergy Int J 2001;1(3):128–45.
[21] Rosen MA, Dincer I, Kanoglu M. Role of exergy in increasing efficiency and sustainability and reducing environmental impact. Energy Policy 2008;36(1):128–37.
[22] Bilgen E. Exergetic and engineering analyses of gas turbine based cogeneration systems. Energy 2000;25(12):1215–29.
[23] Gonçalves P, Angrisani G, Rosselli C, Gaspar AR, Da Silva MG. Comparative energy and exergy performance assessments of a microcogenerator unit in different electricity mix scenarios. Energy Convers Manage 2013;73:195–206.
[24] Feidt M, Costea M. Energy and exergy analysis and optimization of combined heat and power systems. Comparison of various systems. Energies 2012;5:3701–22.
[25] Barelli L, Bidini G, Gallorini F, Ottaviano A. An energetic–exergetic analysis of a residential CHP system based on PEM fuel cell. Appl Energy 2011;88(12):4334–42.
[26] Hepbasli A. A key review on exergetic analysis and assessment of renewable energy resources for a sustainable future. Renew Sustain Energy Rev 2008;12(3):593–661.
[27] Kalogirou SA, Karellas S, Badescu V, Braimakis K. Exergy analysis on solar thermal systems: a better understanding of their sustainability. Renewable Energy 2016;85:1328–33.
[28] Hepbasli A, Akdemir O. Energy and exergy analysis of a ground source (geothermal) heat pump system. Energy Convers Manage 2004;45(5):737–53.
[29] Tsaros TL, Gaggioli RA, Domanski PA. Exergy analysis of heat pumps. ASHRAE Trans 1987;93(2):1781–93.
[30] Crawford RR. An experimental laboratory investigation of second law analysis of a vapor-compression heat pump. ASHRAE Trans 1988;94(2):1491–504.
[31] Bjurström H, Carlsson B. An exergy analysis of sensible and latent heat storage. J Heat Recov Syst 1985;5(3):233–50.
[32] Dincer I. On thermal energy storage systems and applications in buildings. Energy Build 2002;34(4):377–88.
[33] Koca A, Oztop HF, Koyun T, Varol Y. Energy and exergy analysis of a latent heat storage system with phase change material for a solar collector. Renewable Energy 2008;33(4):567–74.
[34] Di Somma M, Yan B, Bianco N, Luh PB, Graditi G, Mongibello L, et al. Operation optimization of a distributed energy system considering energy costs and exergy efficiency. Energy Convers Manage 2015;103:739–51.
[35] Yan B, Di Somma M, Bianco N, Luh PB, Graditi G, Mongibello L, et al. Exergy-based operation optimization of a distributed energy system through the energy-supply chain. Appl Therm Eng 2016;101:741–51.
[36] Mehleri ED, Sarimveis H, Markatos NC, Papageorgiou LG. A mathematical programming approach for optimal design of distributed energy systems at the neighbourhood level. Energy 2012;44:396–1104.
[37] Mehleri ED, Sarimveis H, Markatos NC, Papageorgiou LG. Optimal design and operation of distributed energy systems: application to Greek residential sector. Renewable Energy 2013;51:331–42.
[38] Hawkes AD, Leach MA. Modelling high level system design and unit commitment for a microgrid. Appl Energy 2009;86(7):253–1265.
[39] Omu A, Choudhary R, Boies A. Distributed energy resource system optimisation using mixed integer linear programming. Energy Policy 2013;61:249–66.
[40] Wouters C, Fraga ES, James AM, Polykarpou EM. Mixed-integer optimisation based approach for design and operation of distributed energy systems. In: Power engineering conference (AUPEC), 2014 Australasian Universities IEEE. p. 1–6.
[41] Zhou Z, Zhang J, Liu P, Li Z, Georgiadis MC, Pistikopoulos EN. A two-stage stochastic programming model for the optimal design of distributed energy systems. Appl Energy 2013;103:135–44.

Please cite this article in press as: Di Somma M et al. Multi-objective design optimization of distributed energy systems through cost and exergy assessments. Appl Energy (2017), http://dx.doi.org/10.1016/j.apenergy.2017.03.105

[42] Zhou Z, Liu P, Li Z, Ni W. An engineering approach to the optimal design of distributed energy systems in China. Appl Therm Eng 2013;53:387–96.
[43] Buoro D, Casisi M, De Nardi A, Pinamonti P, Reini M. Multicriteria optimization of a distributed energy supply system for an industrial area. Energy 2013;58:128–37.
[44] Bracco S, Dentici G, Siri S. Economic and environmental optimization model for the design and the operation of a combined heat and power distributed generation system in an urban area. Energy 2013;55:1014–24.
[45] Maroufmashat A, Sattari S, Roshandel R, Fowler M, Elkamel A. Multi-objective optimization for design and operation of distributed energy systems through the multi-energy hub network approach. Ind Eng Chem Res 2016;55 (33):8950–66.
[46] Ramirez-Elizondo LM, Paap GC, Ammerlaan R, Negenborn RR, Toonssen R. On the energy, exergy and cost optimization of multi-energy-carrier power systems. Int J Exergy 2013;13:364–85.
[47] Krause T, Kienzle F, Art S, Andersson G. Maximizing exergy efficiency in multicarrier energy systems. In: Proceedings of IEEE power and energy society general meeting; Minneapolis, USA; 2010 June 25–29.
[48] Lu H, Alanne K, Martinac I. Energy quality management for building clusters and districts (BCDs) though multi-objective optimization. Energy Convers Manage 2014;79:525–33.
[49] ANSI/ASHRAE Standard 55. Thermal environmental conditions for human occupancy; 2013. <http://www.techstreet.com/products/1868610>.
[50] Kotas YJ. The exergy method for thermal plant analysis. reprint ed. Malabar, FL: Krieger; 1995.
[51] Torìo H, Angelotti A, Schmidt D. Exergy analysis of renewable energy-based climatisation systems for buildings: a critical view. Energy Build 2009;41:248–71.
[52] Torìo H, Schmidt D. Framework for analysis of solar energy systems in the built environment from an exergy perspective. Renew Energy 2010;35:2689–97.
[53] Available online: <http://www.ibm.com/developerworks/forums/thread.jspa?threadID=368044>.
[54] Aiying R, Risto L. An effective heuristic for combined heat-and-power production planning with power ramp constraints. Appl Energy 2007;84:307–25.
[55] Weber C, Shah N. Optimisation based design of a district energy system for an eco-town in the United Kingdom. Energy 2011;36(2):1292–308.
[56] Mongibello L, Bianco N, Caliano M, Graditi G. Influence of heat dumping on the operation of residential micro-CHP systems. Appl Energy 2015;160:206–20.
[57] Barbieri ES, Melino F, Morini M. Influence of the thermal energy storage on the profitability of micro CHP systems for residential building applications. Appl Energy 2012;97:714–22.
[58] Bianchi M, De Pascale A, Spina PR. Guidelines for residential micro-CHP systems design. Appl Energy 2012;97:673–85.
[59] ASHRAE International Weather files for Energy Calculations (IWEC weather files). Users manual and CD-ROM, American Society of Heating, Refrigerating and Air-Conditioning Engineers, Atlanta, GA, USA; 2001.
[60] Deloitte. European Energy Market reform – Country Profile: Italy. Available online: <https://www2.deloitte.com/content/dam/Deloitte/global/Documents/Energy-and-Resources/gx-er-market-reform-italy.pdf>.
[61] Trudeau N, Francoeur M. Energy Efficiency indicators for Public Electricity Production from fossil fuels. OECD/IEA; 2008.
[62] Darrow K, Tidball R, Wang J, Hampson A. Catalog of CHP technologies; 2015. Available: <https://www.epa.gov/sites/production/files/2015-07/documents/catalog_of_chp_technologies.pdf>.
[63] Technology Data for Energy Plants. Energinet.dk; 2012. Available: <https://www.energinet.dk/SiteCollectionDocuments/Danske%20dokumenter/Forskning/Technology_data_for_energy_plants.pdf>.
[64] Goldstein L, Hedman B, Knowles D, Freedman SI, Woods R, Schweizer T. Gas-fired distributed energy resource technology characterizations. National Renewable Energy Laboratory; 2003, NREL/TP-620-34783. Available: <http://www.nrel.gov/docs/fy04osti/34783.pdf> <http://www.nrel.gov/docs/fy04osti/34783.pdf>.
[65] Technology Roadmap: Energy-efficient Buildings: Heating and Cooling Equipment. OECD/IEA; 2011. Available: <https://www.iea.org/publications/freepublications/publication/buildings_roadmap.pdf>.
[66] Research on cost and performance of heating and cooling technologies. Final Report. Department of Energy and Climate Change; 2013. Available: <https://www.gov.uk/government/uploads/system/uploads/attachment_data/file/204275/Research_on_the_costs_and_performance_of_heating_and_cooling_technologies__Sweett_Group_.pdf>.
[67] Heat Pumps: Technology Brief. IEA-ETSAP and IRENA; 2013. Available: <https://www.irena.org/DocumentDownloads/Publications/IRENA-ETSAP%20Tech%20Brief%20E12%20Heat%20Pumps.pdf>.
[68] Combined Heat and Power: Policy Analysis and 2011 – 2030 Market Assessment. ICF International, Inc; 2012. Available: <http://www.energy.ca.gov/2012publications/CEC-200-2012-002/CEC-200-2012-002.pdf>.
[69] Thermal Energy Storage: Technology Brief. IEA-ETSAP and IRENA; 2013. Available: <https://www.irena.org/DocumentDownloads/Publications/IRENA-ETSAP%20Tech%20Brief%20E17%20Thermal%20Energy%20Storage.pdf>.

Please cite this article in press as: Di Somma M et al. Multi-objective design optimization of distributed energy systems through cost and exergy assessments. Appl Energy (2017), http://dx.doi.org/10.1016/j.apenergy.2017.03.105